Journal of Medicinal Chemistry

Article

Modulation in selectivity and allosteric properties of small-molecule ligands for CC-chemokine receptors.

Stefanie Thiele, Mikkel Malmgaard-Clausen, Jens Engel-Andreasen, Anne Steen, Pia C. Rummel, Mads C. Nielsen, David E. Gloriam, Thomas M. Frimurer, Trond Ulven, and Mette M. Rosenkilde

J. Med. Chem., **Just Accepted Manuscript** • DOI: 10.1021/jm301121j • Publication Date (Web): 07 Sep 2012

Modulation in selectivity and allosteric properties of small-molecule ligands for CC-chemokine receptors.

Stefanie Thiele[a], Mikkel Malmgaard-Clausen[a†], Jens Engel-Andreasen[b], Anne Steen[a], Pia C. Rummel[a], Mads C. Nielsen[b†], David E. Gloriam[c], Thomas M. Frimurer[d], Trond Ulven[b], and Mette M. Rosenkilde[a*]

[a] Department of Neuroscience and Pharmacology, Faculty of Health and Medical Sciences, The Panum Institute, University of Copenhagen, Blegdamsvej 3, Dk-2200 Copenhagen, Denmark

[b] Department of Physics, Chemistry and Pharmacy, University of Southern Denmark, Campusvej 55, Dk-5230 Odense, Denmark

[c] Department of Drug Design and Pharmacology, Faculty of Health and Medical Sciences, University of Copenhagen, Universitetsparken 2, Dk-2100 Copenhagen, Denmark

[d] The Novo Nordisk Foundation Center for Basic Metabolic Research, Faculty of Health and Medical Sciences, University of Copenhagen, Blegdamsvej 3, Dk-2200 Copenhagen, Denmark

ABSTRACT: Among 18 human chemokine receptors, CCR1, CCR4, CCR5 and CCR8 were activated by metal ions Zn(II) or Cu(II) in complex with 2,2'-bipyridine or 1,10-phenanthroline with similar potencies (EC_{50} from 3.9 to 172 μM). Besides being agonists, they acted as selective allosteric enhancers of CCL3. These actions were dependent on a conserved glutamic acid in TM-7 (VII:06/7.39). A screening of 20 chelator analogs in complex with Zn(II) identified compounds with increased potencies, with **7** reaching highest potency at CCR1 (EC_{50} of 0.85 μM), **20** at CCR8 (0.39 μM) and **8** at CCR5 (1.0 μM). Altered selectivity for CCR1 and CCR8 over CCR5 (**11**, **12**) and a receptor-dependent separation of allosteric from intrinsic properties was achieved (**20**). The pocket similarities of CCR1 and CCR8 contrary to CCR5 as proposed by the ligand-screen were enlightened by computational modeling. These studies facilitate exploration of chemokine receptors as possible targets for therapeutic intervention.

INTRODUCTION

Chemokine receptors belong to class A 7 transmembrane helix (7TM) receptors (also known as G protein-coupled receptors, GPCRs). The 7TM protein family is one of the largest families in the human genome and represents the one most extensively exploited by current drugs. [1,2] The involvement of the chemokine system in numerous pathologies including inflammatory diseases, cancer development, progression and metastasis, and HIV-infection, emphasizes the importance of understanding the biology and pharmacology of this system, and has lead to the development of numerous antagonists for chemokine receptors (e.g. the marketed drugs Maraviroc and Mozobil). [3,4] Here agonists are characterized, but as the path from an agonist to an antagonist could be as short as a methyl group, these data add important information to chemokine receptor ligand design.

The endogenous chemokine system comprises more than 50 ligands and 18 receptors and is characterized by redundancy and promiscuity. [5-7] Many receptors bind several chemokines, and the majority of

chemokines interact with more than one receptor – an obviously challenging phenomenon in drug development. [8] Most chemokines contain four conserved cysteines engaged in two disulfide bridges, a flexible N-terminus before the first cysteine, an N-loop, a 3_{10}-helix, a three-stranded ß-sheet and a C-terminal α-helix. It has repeatedly been reported that the chemokine N-terminus is involved in receptor activation via interaction with the receptor transmembrane region, while the chemokine core interacts with the extracellular receptor domains. [7,9-11] The two first cysteine residues occur in four different sequential patterns that determine the nomenclature by being adjacent to each other (CCL1 to CCL28 [12]), separated by one (CXCL1 to CXCL16) or three amino acid residues (CX_3CL1) or partially missing, i.e. exist as one single cysteine (XCL1 and XCL2). [6]

Metal ions are important for the function of numerous proteins. Zn(II) for instance serves as a part of the active site in metalloenzymes and acts as stabilizer of transcription factors in Zn(II) finger binding motifs. [13] Moreover, zinc-ions are high-affinity modulators of membrane protein function, as shown for the dopamine transporters [14] as well as tachykinin NK3, [15] the nicotinic acetylcholine [16] and ionotropic glutamate receptors. [17] Due to their well-described interaction with proteins, metal ions alone or in complex with chelators have proven very useful in 7TM receptor research during the last decades. [18] The introduction of metal ion sites in for instance the $ß_2$-adrenergic receptor and in CXCR3 have contributed to the understanding of the molecular requirements for receptor activation, and have suggested that an inward movement of the extracellular part of TM-6 towards TM-3 is necessary for agonist-mediated receptor activation. [18-20] The inward movement of helices on the extracellular side comes along with an outward movement of the intracellular parts, [21,22] exposing motifs important for interaction with downstream signaling molecules, such as G proteins. This understanding of receptor activation has indeed been confirmed by the several crystal structures of 7TM receptors in their active and inactive states released during the last years. [23-26]

Although metal ions alone can induce activation in certain wildtype and modified receptors,[15,27-34] linking a hydrophobic molecule such as a chelator to the metal ion potentially improves ligand activity by adding interactions with additional residues (second-site interactions). For instance in CXCR3, an agonistic metal ion chelator site could be built by introduction of a His in TM-3 (position III:05/3.29[35]) that, together with an endogenous Asp in TM-4 (position IV:20/4.60), constituted the metal ion binding site, while the chelator interacted with a Tyr in TM-6 (TyrVI:16/6.51). Importantly, this chelator site was further stabilized by an aromatic zipper consisting of PheIII:08/3.32 and TyrVII:10/7.43, that together with TyrVI:16/6.51 stabilized the inward movement of the extracellular part of TM-6 (with the chelator site) towards TM-3 (with the metal ion binding site) and thus the active receptor conformation.[20]

Interestingly, the existence of naturally occurring agonistic metal ion chelator sites, more precisely Zn(II) or Cu(II) in complex with 2,2'-bipyridine (Bip) or 1,10-phenanthroline (Phe), has been shown in CCR1 and CCR5.[11,39] In these two receptors, the metal ion chelator activities were found to be highly dependent on a Glu located in the top of TM-7 (position TM-VII:06/7.39) between the major (delineated by TM-3 to -7) and the minor binding pocket (delineated by TM-1 to -3 and -7) of the main binding crevice.[40] This Glu is highly conserved among chemokine receptors (74%) while it is found in < 1% of non-chemokine class A 7TM receptors.[41] Importantly, the metal ion chelator complex may emulate other reported structures for chemokine receptor small molecule ligands that, independently of their efficacy, share the motif of one or two centrally located positive charges linked to aromatic/hydrophobic terminals. In most cases, the positively charged groups of the ligands are anchored to the conserved GluVII:06/7.39.[11,39,41-44]

Here the entire group of endogenous chemokine receptors with G protein-mediated signaling including 10 CC-chemokine receptors (CCR1-CCR10), 6 CXC-chemokine receptors (CXCR1-CXCR6) as well as CX_3CR1 and XCR1 were tested for their ability to be activated by the metal ions Zn(II) or Cu(II) in

complex with the chelators 2,2'-bipyridine or 1,10-phenanthroline. CXCR7 was excluded due to no known independent signaling but only CXCR4 modulating effects.[45] CCR1 and CCR5 share chemokine-binding profiles, as both receptors are activated by CCL3 and CCL5, and have both been shown previously to bind metal ion chelator complexes as agonists and positive allosteric enhancers.[11,39] In addition to CCR1 and 5, the metal ion chelators activated CCR8 and CCR4, despite no overlap in chemokine-binding between CCR1/5 and CCR4 or 8, but none of the remaining chemokine receptors. The activity of metal ion chelators was dependent on GluVII:06/7.39 in all four receptors (CCR1, 4, 5 and 8). Further screening of four bipyridine analogs, 13 phenanthroline analogs and three chelators with a new 2,2':6',2''-terpyridine-scaffold in complex with Zn(II) showed that the agonistic potencies of metal ion chelator complexes could be enhanced up to 106-fold as compared to ZnBip and that selectivity could be introduced for CCR1 and CCR8 over CCR5. Intriguingly, a separation between the allosteric and the agonistic properties could be achieved in the new class of 2,2':6',2''-terpyridines, which were pure agonists on CCR1 and pure allosteric modulators of CCR5, a property of special interest for drugs targeting the highly promiscuous chemokine-system.[46,47]

RESULTS

Several CC-chemokine receptors are activated by metal ion chelator complexes. All endogenous chemokine receptors were screened for activation by four selected metal ion chelators Zn(II)- or Cu(II)-ions in complex with 2,2'-bipyridine (Bip) or 1,10-phenanthroline (Phe), abbreviated as ZnBip, ZnPhe, CuBip, CuPhe, by using inositoltriphosphate (IP_3)-turnover measurements in COS-7 cells transiently transfected with the receptor of interest and the promiscuous G protein G_{qi4myr}. In addition to CCR1 and 5,[11,39] also CCR8 was activated with micromolar potencies and efficacies reaching almost the level of the endogenous ligand CCL1 (up to 92%) (Figure 1). As for CCR1 and 5, the phenanthroline complexes dis-

played highest potencies at CCR8 (3.9 μM for ZnPhe and 4.7 μM for CuPhe) as compared to the bipyridine complexes (42 μM for ZnBip and 50 μM for CuBip). Less efficacious (< 50% of endogenous chemokine), but still potent activation was observed in CCR4, where ZnPhe and CuPhe had potencies of 24 μM and 20 μM, respectively, whereas ZnBip and CuBip displayed lower potencies (172 μM and 74 μM, respectively) (Figure 1). Control experiments showing activation of receptors by their endogenous ligands, as well as lack of activity in untransfected cells are provided in Supporting Information 1.

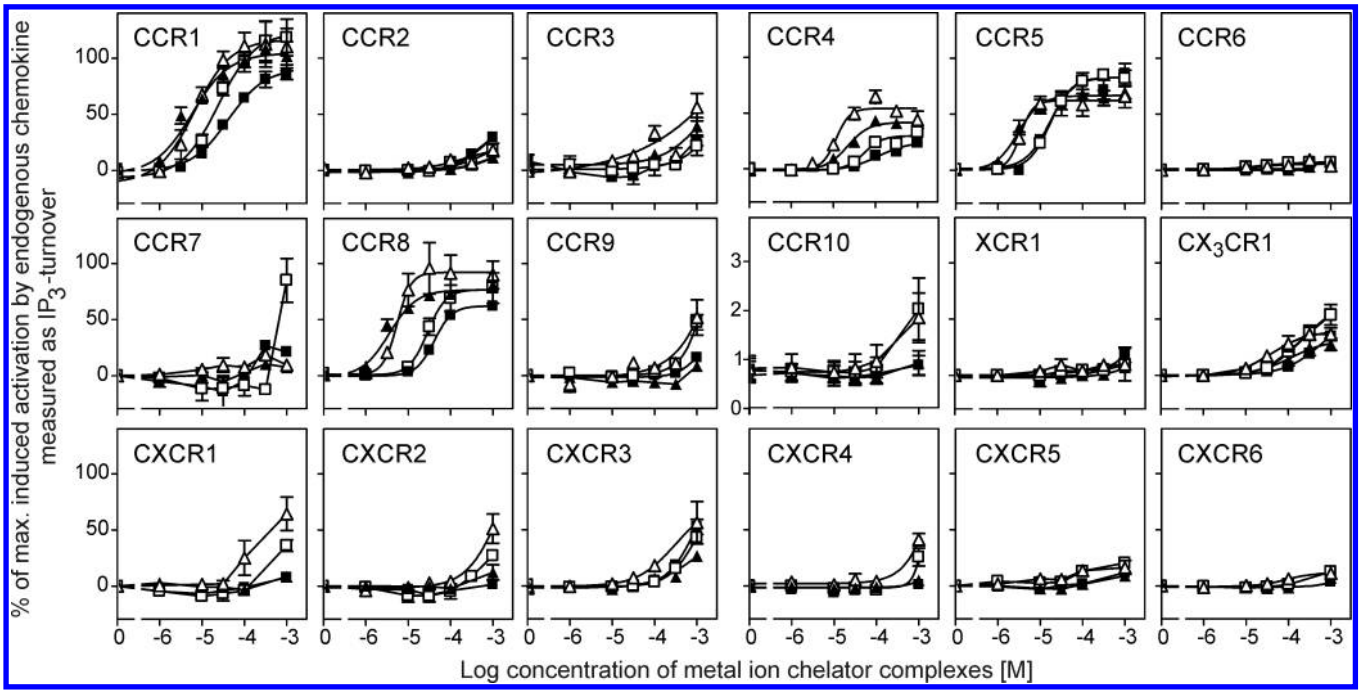

Figure 1. Agonistic activity of the four metal ion chelators ZnBip, ZnPhe, CuBip and CuPhe on all human chemokine receptors (CCR1-10, CXCR1-6, XCR1 and CX_3CR1).

As in CCR1 and 5,[11,39] complex formation between metal ions and chelators was essential for activation in CCR4 and 8 as neither metal ions nor chelators alone could activate the receptors (data not shown). Activation of CXCR1 and CX_3CR1 also appeared, yet with very low potency (Figure 1). In contrast to CCR1 and 5, where the four metal ion chelator complexes acted as allosteric enhancers of ^{125}I-CCL3

binding, [11,39] no enhancement, but low affinity displacement was observed of ^{125}I-CCL1 from CCR8 (Supporting Information 2). [48]

The activity of metal ion chelators depends on a glutamate in TM-7 (VII:06/7.39). As many small molecule ligands for CC-chemokine receptors contain a centrally located positive charge that interacts with GluVII:06/7.39, [41] the role of this residue in CCR8 and CCR4 was explored by Ala-substitution: [E286A]-CCR8 and [E290A]-CCR4. The activities of ZnBip, ZnPhe, CuBip and CuPhe completely depended on this residue in both receptors (as exemplified by CuPhe in Figure 2), in consistency with previous data for CCR1 and 5. [11,39] Despite very low surface expression of [E286A]-CCR8, CCL1 induced a robust activation of this mutant with wt-like potency, while the activity of CCL22 at the well-expressed mutant [E290A]-CCR4 was completely abolished (Supporting Information 3). This indicates that metal ion chelator activity was crucially dependent on GluVII:06/7.39 in all four CC-chemokine receptors (CCR1, 4, 5 and 8).

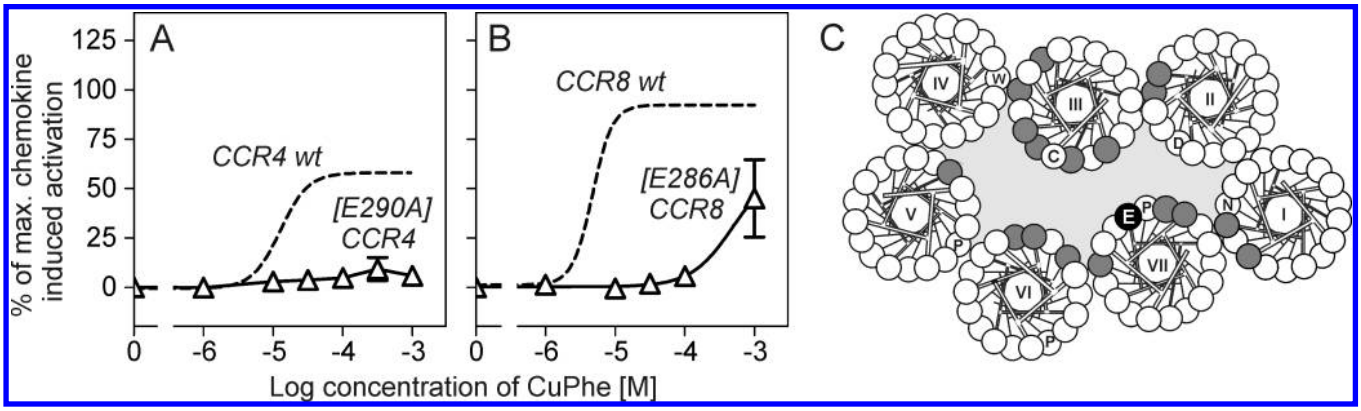

Figure 2. Mutation of GluVII:06/7.39 abrogates metal ion chelator activity.

Phylogenetic clustering of chemokine receptors with an agonistic metal ion chelator site. A phylogenetic analysis based on the entire receptor sequence was performed to investigate the correlation of

receptor primary structure with activation by metal ion chelators (Figure 3A). All four receptors with the agonistic metal ion chelator site (CCR1, 4, 5 and 8) clustered in the same area with the highest similarity between CCR1 and 5. However, also CCR3 and CCR2, which are not activated by these metal ion chelators, were located in the same cluster. A similar correlation with a closer relation of CCR1, 8 and 4 was found when only residues lining the main ligand-binding crevice were analyzed (highlighted in grey in Figure 2C), while the branch-length to CCR5 was longer, indicating structural differences of the ligand-binding site in CCR5 (Figure 3B). Furthermore, although GluVII:06/7.39 is required for activation by metal ion chelators (Figure 2), [11,39] it is not sufficient, as it is present in most chemokine receptors (except for CCR7, 9, 10, CXCR3 and XCR1), and also in CCR2 and CCR3 where no metal ion chelator activities were observed despite close similarity to CCR5 and CCR1.

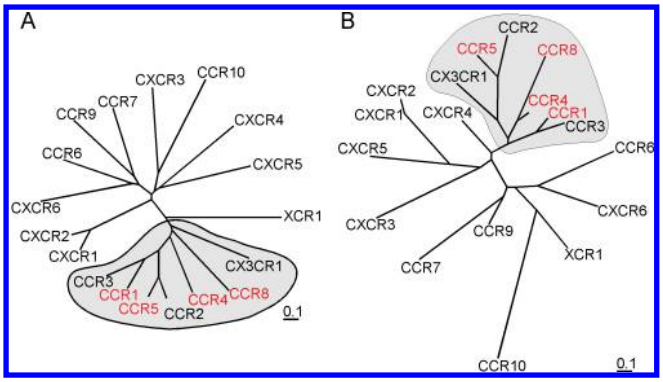

Figure 3. Phylogenetic and chemogenomic analysis of chemokine receptors.

Large variation in Zn(II)-affinities among 22 different metal ion chelators. To improve the ligands activities, a series of chelator analogs were introduced comprising five bipyridines (Chart 1A, Bip and **1**-**4**), 14 phenanthrolines (Chart 1B, Phe and **5**-**17**) and three terpyridines (Chart 1C, 2,2':6',2''-terpyridine (**18**) and analogs **19** and **20**). Substitutions comprised methyl-, methoxy-, hydroxyl-, formyl-groups and

halogens. First, the ability of the chelators to bind Zn(II) was tested in a fluorescence-based assay with the Zn(II)-sensitive fluorophore Fluozin3 under the same conditions as the functional IP_3-turnover measurements (Figure 4, Table 1). [49]

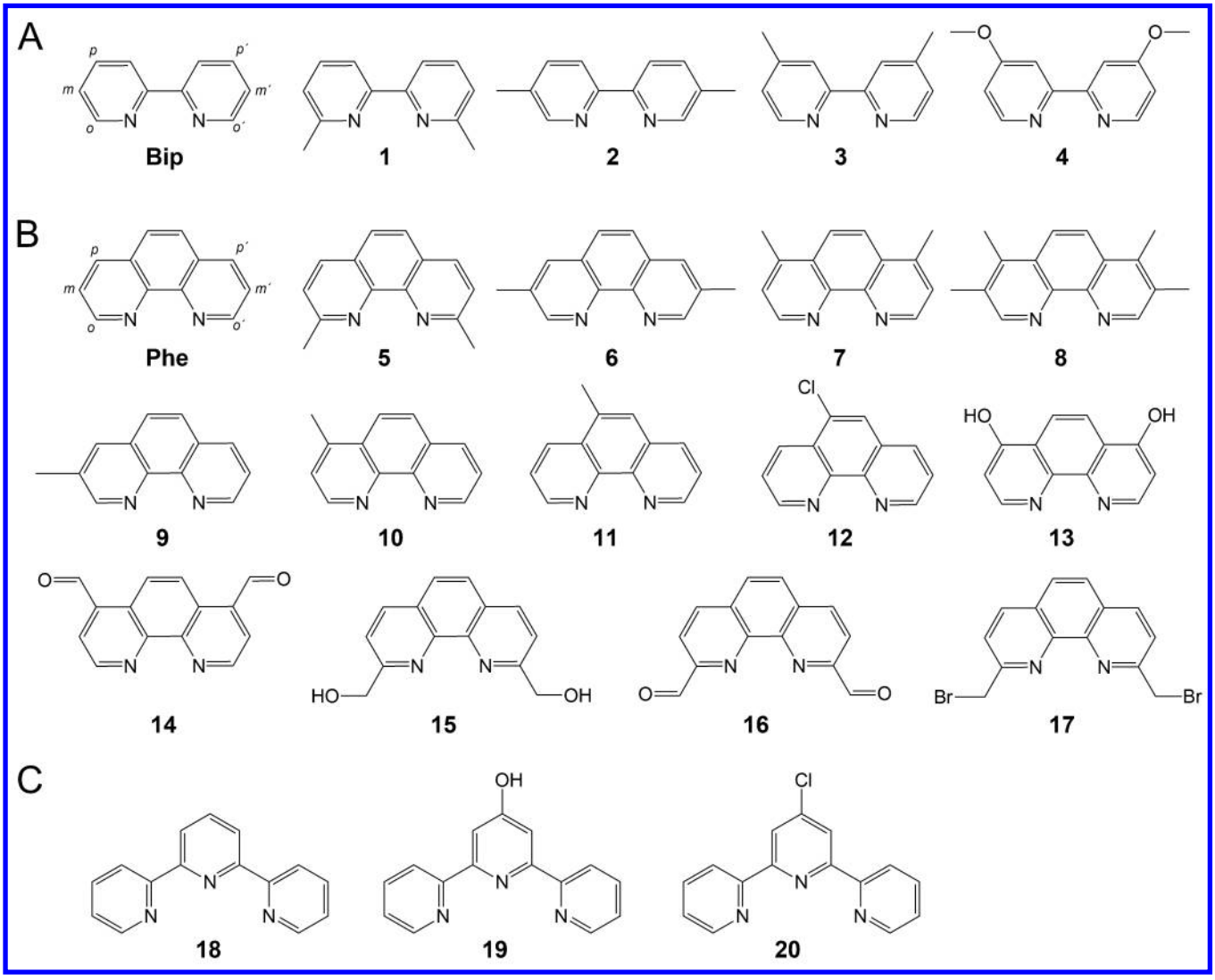

Chart 1. Structures of the chelator analogs.

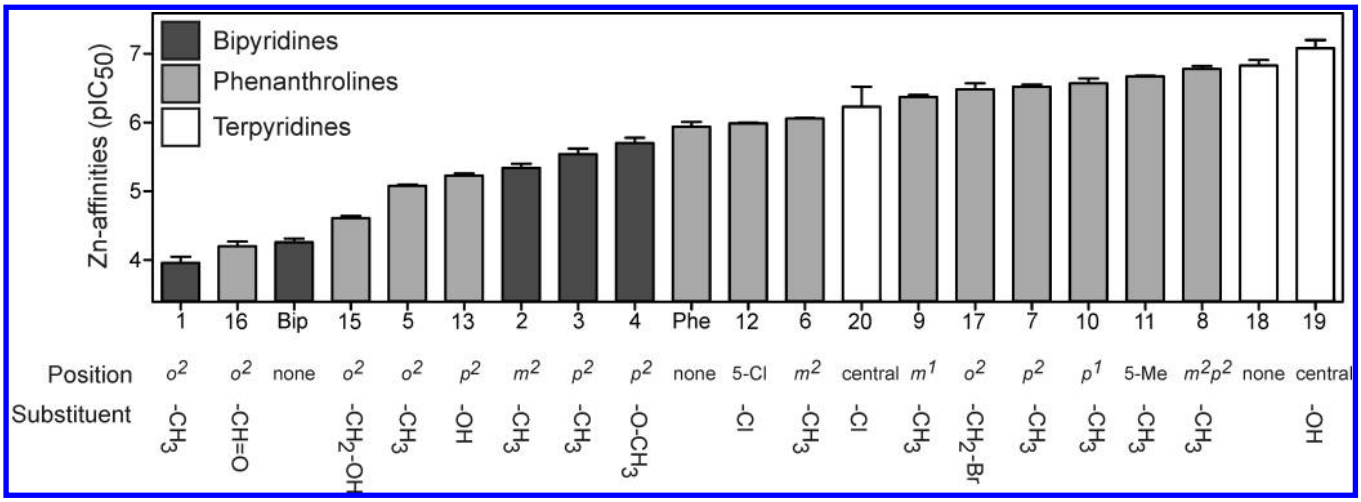

Figure 4. The chelators affinities for Zn(II).

Focusing only on the chelator scaffold, it was found that 2,2':6',2''-terpyridine (**18**) had a higher Zn(II)-affinity than phenanthroline and bipyridine, in agreement with the higher number of coordinating nitrogens in terpyridines. Furthermore, phenanthrolines display higher Zn(II)-affinities as compared to bipyridines. Different chemical substituents had different effects on the Zn(II)-affinity of the chelators. Electron-donating groups, such as methyl- (**2**, **3**, **6**, **9**, **7**, **10**, **11** and **8**) or methoxy-groups (**4**), led to a higher electron density at the ring-nitrogens and consequently to a higher Zn(II)-affinity. Thus, the methyl-substituted phenanthroline analogs **8**, **11**, **10**, **7** and **9** were among the compounds with highest Zn(II)-affinities, only exceeded by the two terpyridine compounds **18** and **19**. Also substitution of Phe with bromomethyl-groups in the *ortho*-position (**17**) resulted in an increased Zn(II)-affinity, possibly owing to a direct interaction of the bromines with the metal ion. For other *ortho*-methyl substituted chelators, decreased Zn(II)-affinities were observed (**1**, **5**), as in fact also for *ortho*-substitutions with formyl- (**16**) or hydroxymethyl-groups (**15**). As expected, *para*-methyl-substituted chelators (**3** and **7**) displayed a higher Zn(II)-affinity than *meta*-methyl substituted chelators (**2** and **6**) and 3,4,7,8-tetramethyl-phenanthroline (**8**) displayed the highest affinity among all tested phenanthrolines. There was no ex-

pected increase in Zn(II)-affinity by addition of hydroxyl-groups in *para*-position of Phe (**13**), instead this compound was found to have a 5.4-fold decreased Zn(II)-affinity as compared to Phe. The electron-donating nature of hydroxyl-groups was however confirmed by 4'-hydroxy-terpyridine (**19**) which had a Zn(II)-affinity that was ~ 2-fold higher compared to the unsubstituted terpyridine (**18**). It is suggested that this very high affinity of 83 nM originated from the deprotonation of the hydroxyl-group, in its keto-tautomeric form resulting in a formal negative charge at the central ring-nitrogen.

Finally, the electron-withdrawing formyl (**16**), chloro (**12**, **20**) or hydroxymethyl substitutents (**15**) resulted in compounds with lower Zn(II)-affinities than methyl-substituted chelators (Table 1). A Zn(II)-coordinating role might be expected for the *ortho*-hydroxymethyl groups in **15** (similarly to 17). However, a 23-fold lower Zn(II)-affinity was observed as compared to Phe.

Table 1. The chelators affinity to Zn(II) and their potency at activating CCR1, CCR8 and CCR5.

					Affinity to Zn(II)			CCR1					CCR8					CCR5				
Scaffold	Pos.	Subst.	Full name		IC_{50} ± SEM *(log)*	IC_{50} *(μM)*	(n)	Potency EC_{50} ± SEM *(log)*	*(μM)*	F_{lig}	Efficacy E_{max} ± SEM *(fold)*	(n)	Potency EC_{50} ± SEM *(log)*	*(μM)*	F_{lig}	Efficacy E_{max} SEM *(fold)*	(n)	Potency EC_{50} ± SEM *(log)*	*(μM)*	F_{lig}	Efficacy E_{max} SEM *(fold)*	(n)
	Bip		2,2'-Bipyridine		-4.3 ± 0.05	54	(4)	-4.5 ± 0.05	34	**1.0**	5.2 ± 0.20	(34)	-4.4 ± 0.03	42	**1.0**	3.3 ± 0.14	(39)	-4.7 ± 0.05	19	**1.0**	5.8 ± 0.33	(20)
	Phe		1,10-Phenanthroline		-5.9 ± 0.07	1.1	(4)	-5.2 ± 0.07	5.9	**1.0**	5.5 ± 0.32	(30)	-5.4 ± 0.05	3.9	**1.0**	3.5 ± 0.13	(37)	-5.3 ± 0.08	4.9	**1.0**	5.0 ± 0.35	(20)
Bipyridines	1	o^2	$-CH_3$	6,6'-Dimethyl-2,2'-bipyridine	-4.0 ± 0.09	110	(4)	-4.9 ± 0.33	12	**2.8**	3.2 ± 0.76	(4)	-5.3 ± 0.24	4.8	**8.7**	1.3 ± 0.06	(4)	> -3	> 1000			(4)
	2	m^2	$-CH_3$	5,5'-Dimethyl-2,2'-bipyridine	-5.3 ± 0.06	4.5	(4)	-4.8 ± 0.08	17	**2.0**	4.9 ± 0.45	(7)	-5.1 ± 0.06	7.5	**5.6**	2.9 ± 0.20	(5)	-5.6 ± 0.05	2.3	**8.2**	6.4 ± 0.83	(3)
	3	p^2	$-CH_3$	4,4'-Dimethyl-2,2'-bipyridine	-5.5 ± 0.08	2.9	(4)	-5.4 ± 0.07	3.6	**9.4**	5.1 ± 0.41	(6)	-5.5 ± 0.06	3.3	**13**	3.1 ± 0.29	(4)	-4.9 ± 0.04	11	**1.7**	5.1 ± 0.70	(3)
	4	p^2	$-O-CH_3$	4,4'-Dimethoxy-2,2'-bipyridine	-5.7 ± 0.08	2.0	(4)	-5.0 ± 0.14	10	**3.3**	5.5 ± 0.34	(7)	-5.3 ± 0.03	5.4	**7.7**	3.0 ± 0.19	(3)	-4.7 ± 0.13	22	**0.87**	4.7 ± 0.32	(3)
Phenanthrolines	5	o^2	$-CH_3$	2,9-Dimethyl-1,10-phenanthroline	-5.1 ± 0.02	8.4	(3)	-5.8* ± 0.09	1.6	**3.8**	3.7 ± 0.67	(4)	> -3	> 1000			(4)	-4.2* ± 0.13	67	**0.07**	6.4 ± 1.2	(3)
	6	m^2	$-CH_3$	3,8-Dimethyl-1,10-phenanthroline	-6.1 ± 0.01	0.87	(3)	-5.3 ± 0.13	4.9	**1.2**	6.1 ± 0.30	(4)	-5.2 ± 0.12	7.0	**0.56**	3.5 ± 0.22	(3)	-5.7 ± 0.05	1.9	**2.7**	6.7 ± 0.14	(4)
	7	p^2	$-CH_3$	4,7-Dimethyl-1,10-phenanthroline	-6.5 ± 0.03	0.31	(3)	-6.1 ± 0.14	0.85	**7.0**	4.9 ± 0.06	(3)	-6.3 ± 0.13	0.52	**7.5**	2.6 ± 0.30	(4)	-5.6 ± 0.06	2.6	**1.9**	5.2 ± 0.87	(3)
	8	m^2p^2	$-CH_3$	3,4,7,8-Tetramethyl-1,10-phenanthroline	-6.8 ± 0.04	0.16	(4)	-5.8 ± 0.09	1.5	**3.9**	4.3 ± 0.33	(4)	-6.3 ± 0.14	0.48	**8.2**	3.1 ± 0.42	(4)	-6.0 ± 0.04	1.0	**5.0**	6.3 ± 0.41	(3)
	9	*m*	$-CH_3$	3-Methyl-1,10-phenanthroline	-6.4 ± 0.03	0.43	(3)	-5.9 ± 0.09	1.3	**4.5**	6.8 ± 0.37	(4)	-6.2 ± 0.32	0.67	**5.9**	3.8 ± 0.08	(3)	-5.7 ± 0.18	2.2	**2.2**	6.5 ± 0.23	(4)
	10	*p*	$-CH_3$	4-Methyl-1,10-phenanthroline	-6.6 ± 0.07	0.27	(4)	-6.0 ± 0.03	1.0	**6.2**	4.9 ± 0.43	(3)	-6.2 ± 0.13	0.67	**5.9**	3.4 ± 0.43	(4)	-5.7 ± 0.03	1.8	**2.7**	5.5 ± 0.89	(3)
	11	5	$-CH_3$	5-Methyl-1,10-phenanthroline	-6.7 ± 0.01	0.21	(3)	-5.7 ± 0.04	1.8	**3.3**	4.7 ± 0.46	(3)	-5.7 ± 0.11	2.0	**1.9**	2.6 ± 0.20	(4)	> -3	> 1000			(3)
	12	5	-Cl	5-Chloro-1,10-phenanthroline	-6.0 ± 0.01	1.0	(3)	-5.7 ± 0.02	2.0	**3.0**	4.6 ± 0.32	(3)	-5.5 ± 0.06	3.0	**1.3**	2.7 ± 0.39	(4)	> -3	> 1000			(3)
	13	p^2	-OH	4,7-Dihydroxy-1,10-phenanthroline	-5.2 ± 0.03	5.9	(3)	> -4	> 100			(3)	-4.1 ± 0.16	86	**0.48**	1.9 ± 0.06	(3)	> -3	> 1000			(3)
	14	p^2	-CH=O	4,7-Diformyl-1,10-phenanthroline	not tested			-5.3 ± 0.10	5.0	**1.2**	4.5 ± 0.16	(4)	-4.8 ± 0.11	15	**0.26**	3.0 ± 0.07	(3)	-5.0 ± 0.09	10	**0.48**	2.5 ± 0.23	(4)
	15	o^2	$-CH_2-OH$	2,9-(Bishydroxymethyl)-1,10-phenanthroline	-4.6 ± 0.03	25	(3)	-5.0 ± 0.05	10	**0.57**	3.2 ± 0.34	(5)	> -3	> 1000			(4)	> -3	> 1000			(4)
	16	o^2	-CH=O	1,10-Phenanthroline-2,9-dicarbaldehyde	-4.2 ± 0.07	64	(3)	-4.9 ± 0.36	13	**0.47**	2.2 ± 0.30	(3)	> -3	> 1000			(3)	> -3	> 1000			(3)
	17	o^2	$-CH_2-Br$	2,9-(Bisbromomethyl)-1,10-phenanthroline	-6.5 ± 0.09	0.33	(3)	-4.8 ± 0.18	15	**0.39**	3.9 ± 0.40	(4)	> -3	> 1000			(3)	> -3	> 1000			(4)
Terpyridines	18			2,2':6',2''-Terpyridine	-6.8 ± 0.08	0.15	(3)	-4.2 ± 0.15	64	**0.53**	4.7 ± 0.65	(6)	-5.3 ± 0.11	4.9	**8.4**	2.7 ± 0.24	(3)	-4.5 ± 0.06	29	**0.67**	4.9 ± 0.48	(3)
	19	central	-OH	4'-Hydroxy-2,2':6',2''-terpyridine	-7.1 ± 0.12	0.08	(3)	> -3	> 1000			(3)	> -3	> 1000			(3)	> -3	> 1000			(4)
	20	central	-Cl	4'-Chloro-2,2':6',2''-terpyridine	-6.2 ± 0.29	0.59	(3)	-5.9 ± 0.09	1.2	**28**	5.7 ± 0.40	(8)	-6.4 ± 0.18	0.39	**106**	3.4 ± 0.22	(5)	> -3	> 1000			(5)

Improvement of intrinsic activity and allosteric properties. The complete series of chelator analogs (Chart 1) in complex with Zn(II) was tested for functional properties in CCR1, 5 and 8 (CCR4 was excluded due to the lower potencies and efficacies (Figure 1)). Comparing the potencies for the Zn(II)-chelator complexes on the three receptors with the Zn(II)-affinities of the chelators revealed a positive correlation (Figure 5 and Supporting Information 4).

The methyl-substituted phenanthroline analogs that were among the compounds with highest Zn(II)-affinities (**8**, **11**, **10**, **7**, **9** and **6**, ranked after affinities) (Figure 4, light grey columns), also displayed the highest potencies for all three receptors (Figure 5), except for **11** that was inactive in CCR5. In fact all methyl-substituted phenanthroline analogs activated the receptors with high potencies (in contrast to **19**) showing that no saturation of the metal ion occurred. This might be attributed to the lower number of coordinating nitrogens of phenanthrolines compared to terpyridines. Similarly, addition of methyl- (**3**, **2**) or methoxy-groups (**4**) to bipyridine led to increased potencies as compared to the unsubstituted bipyridine.

Chelators with substitutions in the *ortho*-position (**17**, **5**, **15**, **16** and **1**) had lowered Zn(II)-affinities (except for **17**, see above), and were impaired in activity with no action on CCR5. Only **1** activated CCR1 and CCR8, whereas **16** and **15** activated CCR1, yet with low efficacy, thus being somewhat affected by the *ortho*-substitutions (Figure 5, Table 1).

The terpyridines **18** and **19** displayed low potencies (**18**) or a complete inability (**19**) to activate the receptors, despite very high Zn(II)-affinities. Introduction of the electron-withdrawing 4-chloro substituent on terpyridine (**20**) resulted in high Zn(II)-affinity, albeit lower than **18** and **19** (Figure 4), and high potency in CCR1 and CCR8 (EC_{50} values of 1.2 μM and 0.39 μM, respectively). Interestingly, this compound had no activity on CCR5 (see below).

Finally, 4,7-diformyl-1,10-phenanthroline (**14**) activated all three receptors similarly to Phe. Addition of hydroxyl-groups at the same positions (**13**) abolished all activity, which might be explained by the decreased Zn(II)-affinity of the chelator, but could also be caused by the hydrophilic character of the substituent and disfavored interaction with the receptor. As mentioned in more details below, similarly to the 5-methyl-substituted Phe (**11**), 5-chloro-substituted Phe (**12**) was able to activate CCR1 and 8, but not CCR5.

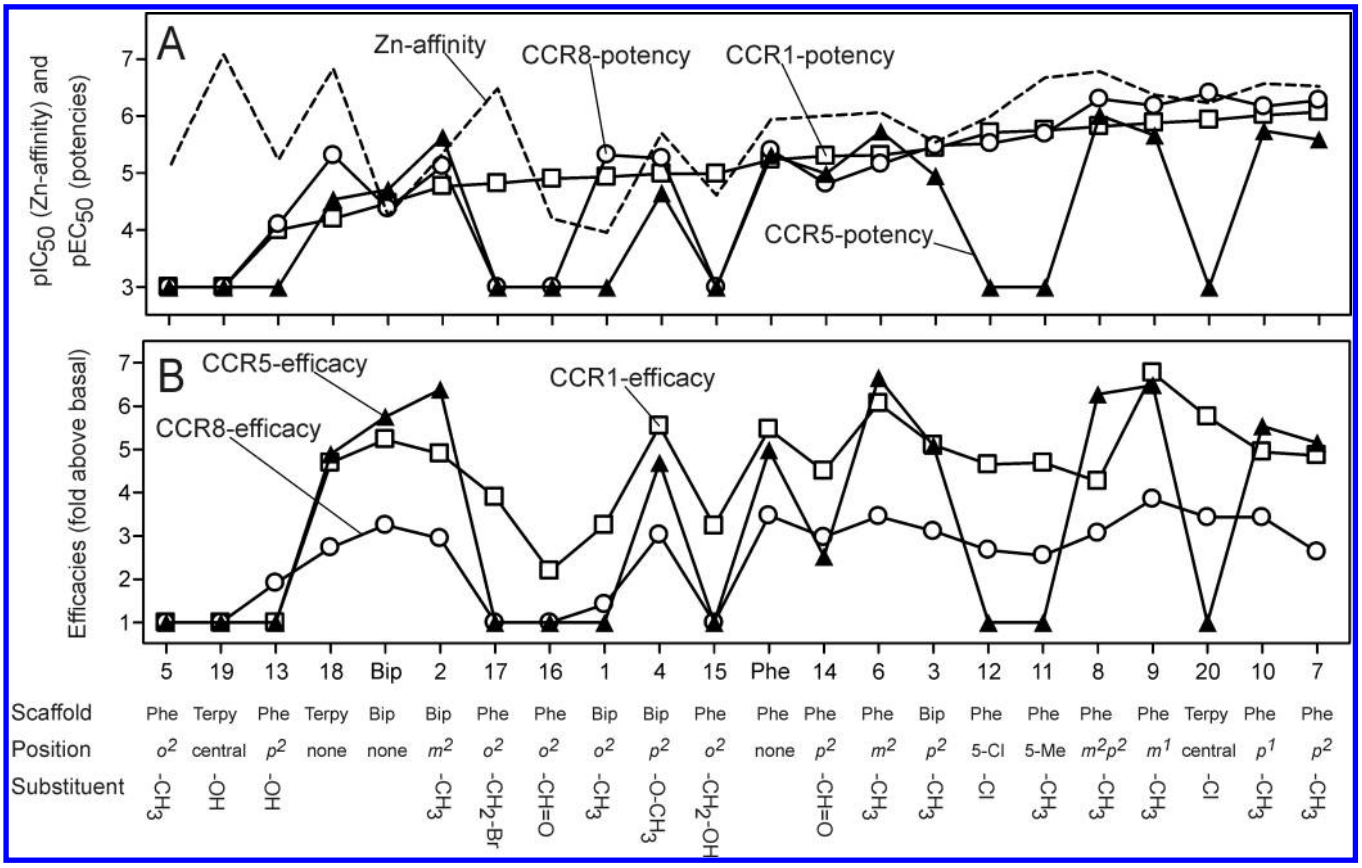

Figure 5. Zn(II)-affinities and potencies of the chelators in complex with Zn(II) are positively correlated.

CCR5 has a differently shaped binding pocket than CCR1 and 8. The broad analysis of all Zn(II)-chelated complexes uncovered that the top-five most potent compounds were identical in CCR1 and 8: 4,7-dimethyl-phenanthroline (**7**), 4-methyl-phenanthroline (**10**), 4'-chloro-terpyridine (**20**), 3-methyl-phenanthroline (**9**) and 3,4,7,8-tetramethyl-phenanthroline (**8**) with EC_{50} values from 0.85 μM to 1.5 μM in CCR1 with **7** being most potent, and EC_{50} values from 0.39 μM to 0.67 μM in CCR8 with **20** having highest potency (Table 1). In contrast, the picture was somewhat different in CCR5, where the five most potent compounds were **8**, **10**, **6**, **9** and **2** with EC_{50} values from 1.0 μM to 2.3 μM, and **8** being most potent (Table 1).

This was a general trait, as comparison of potencies and efficacies not only of the top five, but of all Zn(II)-chelator complexes uncovered a close correlation of CCR1 and 8 contrary to CCR5. Both in respect of potency and efficacy, CCR1 and 8 followed each other, with only few exceptions as for instance the unsubstituted terpyridine (**18**) that had an 8.6-fold increased potency as compared to ZnBip at CCR8 while its potency was unchanged (or in fact slightly decreased) at CCR1 (Figure 5). In comparison to CCR5 remarkable differences were found. 4,4'-Dimethyl-bipyridine (**3**) with methyl-substitutions in *para*-position had potencies that were 9.4- and 13-fold higher than that of ZnBip at CCR1 and CCR8, respectively, while it had a potency similar to ZnBip at CCR5. The opposite was found for *meta*-substituted 5,5'-dimethyl-bipyridine (**2**), which was 8.2-fold more potent at CCR5, but less improved at CCR1 and CCR8 (2.0- and 5.6-fold increased EC_{50}, respectively) (Figure 6A-C). Phenanthrolines with substitutions at position 5 (5-methyl-phenanthroline (**11**) and 5-chloro-phenanthroline (**12**)) lacked activity on CCR5, but activated CCR1 and 8 with potencies similar to or slightly better than ZnPhe (Figure 6E-G). Finally, terpyridine compound **20** did not activate CCR5, but CCR1 and 8 with very high potencies. A similar trait was observed for **18** (Figure 6I-K, Table 1). Importantly, non of the metal ion chelator complexes

could activate untransfected cells as presented by ZnBip, ZnPhe, Zn-**2**, -**3**, -**11**, -**12**, -**18** and -**20** in Figure 6 D, H and L.

In summary, chelators with central steric bulk, i.e. large chelators such as terpyridines or phenanthrolines with substitutions at the central ring do not activate CCR5, whereas the elongated (e.g. *meta*-substituted bipyridines as compared to *para*-substituted) chelators are superior at CCR5 activation as compared to CCR1 and 8. The observed similarity between CCR1 and 8 was in line with the phylogenetic analysis based on residues lining the cavity around GluVII:06/7.39, where these two receptors were located closer to each other than to CCR5 (Figure 3B).

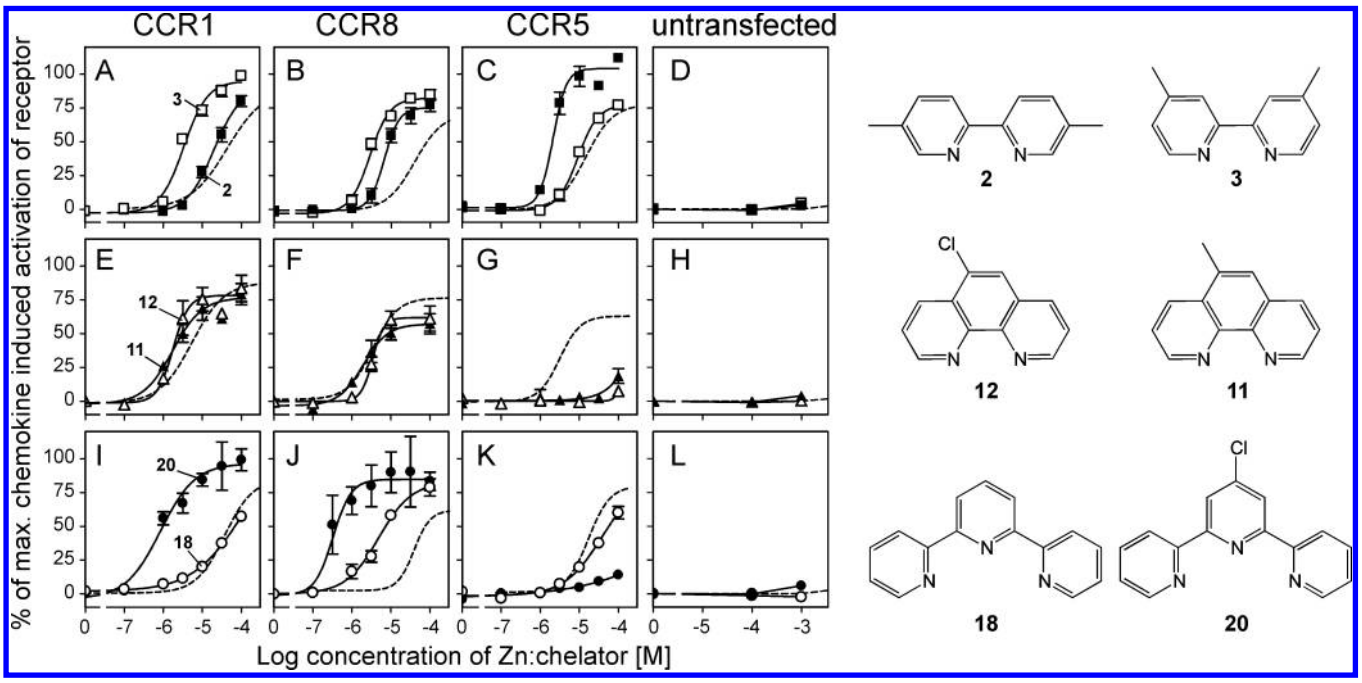

Figure 6. CCR1 and CCR8 are similar, but different from CCR5.

Functional variations correspond to structural differences between CCR1 and 8 on one side and CCR5 on the other. Receptor models of all three receptors were built based on the crystal structure of CXCR4 [50] but with the intracellular parts of TM-5 to -7 adjusted to an active conformation based on the crystal structure of opsin, [23] and extracellular parts of helices aligned to active β_2-adrenergic receptor structures (see methods). [25,26] The shape of the main binding crevices in these models showed three major differences between CCR1/8 and CCR5 (Figure 7). First, the major binding pocket of CCR5 was much deeper (z-dimension) and wider (x/y-dimension) than in CCR1/8. Second, this part of the binding crevice was in CCR5 extended to an area between TM-4 and TM-5, which appeared more closed in CCR1 and 8. Finally, also in the part of the binding crevice between TM-1 to -3 and -7 were found differences in the pocket extension, with this pocket being narrower at the side of TM-1 and -2 in CCR5, but more open between TM-1 and -7 as compared to the pockets of CCR1 and 8. These structural differences correlate well with the functional differences between CCR1 and 8 in comparison to CCR5.

Figure 7. Models of receptors CCR1, CCR8 and CCR5 emphasize structural differences of these receptors.

Terpyridines display altered pharmacodynamic properties. Due to the positive allosteric effects of ZnBip, ZnPhe, CuBip and CuPhe on CCL3 binding in CCR1 and CCR5, [11,39] a selection of chelators presented in this study was tested for their ability to enhance ^{125}I-CCL3-binding to both receptors (Table 2). While the affinities of the bipyridine and phenanthroline analogs in most cases were not increased as compared to the control compounds ZnBip or ZnPhe, and were thus in striking contrast to the enhanced potencies of most of these compounds (Figure 5, Table 1), an even more surprising pharmacology was identified for the terpyridine compounds **18** and **20** (Figure 8). While in particular **20** acted as potent agonist on CCR1, both compounds failed to show allosteric enhancement of ^{125}I-CCL3 binding to CCR1 (Figure 8A, Table 2). Consequently, with **18** and **20**, two highly potent agonists *without* allosteric effects were identified for CCR1. The opposite was seen for CCR5, where **18**, with a potency similar to ZnBip, enhanced ^{125}I-CCL3 binding with an IC_{50} of 25 μM (3.4-fold increased affinity as compared to ZnBip) and an efficacy similar to ZnBip. Compound **20**, with absolutely no CCR5 activity, had an even higher affinity of 8.1 μM (10-fold increased as compared to ZnBip) and enhanced ^{125}I-CCL3 binding to ~ 60% of ZnBip (Figure 8B). Therefore, with **20** allosteric activity was completely and receptor-dependently separated from intrinsic agonistic activity.

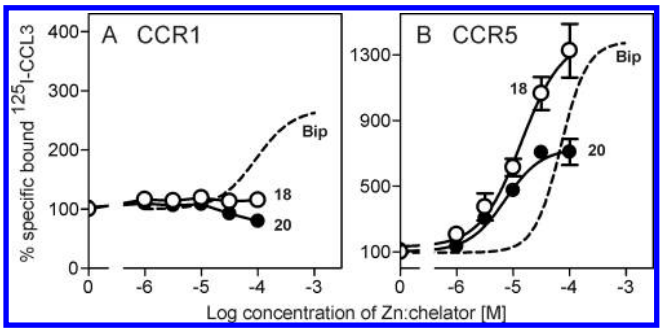

Figure 8. Test of the new class of 2,2':6',2''-terpyridines in binding of ^{125}I-CCL3 to CCR1 and CCR5.

Table 2. Test of the chelator analogs in complex with Zn(II) in competition binding experiments of ^{125}I-CCL3 to CCR1 and CCR5.

	CCR1				CCR5			
	IC50 log ± SEM	(μM)	over basal % ± SEM	(n)	IC50 log ± SEM	(μM)	over basal % ± SEM	(n)
CCL3	-8.1 ± 0.09	0.01	100 ± 0.0	(5)	-7.9 ± 0.17	0.01	100 ± 0.0	(5)
Bip	-3.9 ± 0.13	126	253 ± 46	(4)	-4.1 ± 0.09	84	849 ± 130	(4)
Phe	-4.1 ± 0.17	74	335 ± 18	(3)	-4.3 ± 0.13	53	698 ± 129	(4)
1	No effect			(3)	-3.3 ± 0.13	511	1000 ± 392	(3)
2	-3.7 ± 0.18	204	283 ± 5.5	(3)	-3.7 ± 0.09	206	1015 ± 308	(4)
3	-4.0 ± 0.12	101	243 ± 42	(4)	-3.5 ± 0.03	337	826 ± 209	(4)
4	-3.7 ± 0.12	179	226 ± 54	(3)	-2.8 ± 0.14	1511	751 ± 226	(3)
5	> -3	> 1000		(2)	-4.5 ± 0.25	30	573 ± 29	(2)
6	not determined				not determined			
7	-4.0 ± 0.05	112	528 ± 215	(2)	-3.5 ± 0.04	300	503 ± 122	(2)
8	-3.8 ± 0.10	171	319 ± 13	(2)	No effect			(2)
9	not determined				not determined			
10	-3.6 ± 0.02	261	526 ± 217	(2)	-4.2 ± 0.18	66	675 ± 260	(2)
11	-3.9 ± 0.10	119	319 ± 13	(2)	No effect			(2)
12	-5.3 ± 0.05	5.1	373 ± 34	(3)	No effect			(3)
13	No effect			(2)	> -3	> 1000		(2)
14	> -3	> 1000		(2)	> -3	> 1000		(2)
15	> -3	> 1000		(2)	-3.2 ± 0.02	587	692 ± 287	(2)
16	-5.3 ± 0.23	4.8	361 ± 151	(2)	-3.9 ± 0.17	128	596 ± 217	(2)
17	> -3	> 1000		(2)	-3.7 ± 0.72	205	613 ± 50	(2)
18	No effect			(5)	-4.6 ± 0.16	25	769 ± 143	(5)
19	No effect			(2)	-3.3 ± 0.04	519	775 ± 160	(2)
20	No effect			(4)	-5.1 ± 0.03	8.1	516 ± 102	(4)

DISCUSSION AND CONCLUSION

A broad screen for an agonistic metal ion chelator site among all endogenous chemokine receptors uncovered such a site in CCR1, 4, 5 and 8. The metal ion chelator activity was dependent on GluVII:06/7.39 in the center of the main binding crevice. Further testing of 22 chelators, comprising three different chelator scaffolds (bipyridine, phenanthroline and terpyridine) and with variations in substituents, showed that by rather simple chemical modifications the potencies of the Zn(II)-chelator complexes could be increased up to 106-fold. This increase was in many cases related to an enhanced Zn(II)-affinity. It was also possible to gain selectivity between CCR1 and 8 vs. CCR5 and to modulate the allosteric properties of this class of ligands from being ago-allosteric modulators to being agonists without allosteric properties in CCR1 and simultaneously to being allosteric modulators with no intrinsic activity in CCR5.

Engineered and naturally occurring metal ion binding sites in 7TM receptors.

Because of their well-defined size and coordination geometry, metal ions have proven to be useful tools for structure-function studies. Initially, an antagonistic Zn(II)-site based on the binding site of the antagonist CP96-345 was created in the NK1 receptor between the endogenous His[197] in TMV:05/5.39 and introduced histidines at positions V:01/5.35 and VI:24/6.59. [27] This Zn(II)-site could also be introduced in the κ-opioid receptor. [28] The first example of a site conferring intrinsic (agonist independent) activity to a metal ion was in the CXC-chemokine receptor ORF74, where a Zn(II)-site was created between His residues introduced in the top of TM-5 (V:01/5.35 and V:05/5.39). Via this site, Zn(II) displayed inverse agonistic single digit micromolar potency and additionally gained positive allosteric effects on CXCL1 binding at higher concentrations. [29,33] At exactly the same, yet naturally occurring site in the NK3 receptor, Zn(II) acted as an allosteric enhancer of the agonist (MePhe[7])neurokinin. [15] Later, agonistic metal ion (chelator) sites were constructed in the NK1 [30] and β_2-adrenergic receptor [51] (between

TM-3, -6 and -7), and in CXCR3 (between TM-3, -4 and -6), where an inward movement of the extracellular part of TM-6 accounted for the formation of the metal ion binding site – findings that resulted in the formulation of a model of class A 7TM receptor activation, which proposed a concerted inward- and outward-movement of the extra- and intracellular parts of TM-6, respectively. [18-20] In addition to the NK3 receptor, [15] *endogenous sites* for metal ions alone have been identified in GPR39 [34] and in the melanocortin (MC)1 and MC4 receptors. [52] These sites were located in different areas, for instance between the receptor N-terminus and ECL3 in GPR39 [34] and between Cys^{271} in ECL2 and AspIII:05 in MC1 and 4. [52] In CCR1 and CCR5 GluVII:06/7.39 has been identified as essential for metal ion chelator mediated activation. [11,39] The same dependency of GluVII:06/7.39 was found for the metal ion binding sites identified in CCR4 and 8 in the present study (Figure 1 and 2). However, in CXCR3, where GluVII:06 is missing, the metal ion site was constructed between residues in TM-3 and -4 (HisIII:05/3.29, substituted from Gly, and AspIV:20/4.60). [20] Importantly, despite the different location of the metal ion binding site in the four wt receptors CCR1, 4, 5, 8 and the engineered CXCR3, chelators complexed to the metal ions were necessary for the agonistic action by providing second-site interactions to the otherwise silent metal ion binding sites, and thereby constrain the receptor in active conformations. [11,20]

Affinity of the chelators to Zn(II) is limiting for the potency of the metal ion chelator complex. The affinity of the chelators to Zn(II) could be modulated by the introduction of electron-withdrawing or -donating substituents (Figure 4). Generally, a positive correlation between Zn(II)-affinity and receptor activating potency was observed (Supporting Information 4). However, in certain cases (**3** and **2**), the potency of a ligand seemed limited by its Zn(II)-affinity (Figure 5). One strategy for improving the potency of a Zn(II)-chelator complex therefore is to increase the strength of the chelator. It should however be avoided to saturate the metal ions coordination sites by the chelator, which would prevent interaction

with the receptor as observed for the chelators terpyridine (**18**) and 4'-hydroxy-terpyridine (**19**). Also the cyclam-containing CXCR4-antagonists Mozobil (AMD3100) and analogs have the ability to chelate metal ions, which increase their potency. As for the chelators presented here, the potency-increase of Mozobil was directly correlated to the incorporated ion´s chelation enthalpy for acetate, which reflected the affinity between chelator and ion. [53] That chelation of the metal ion via four nitrogens in such a cyclam-ring did not "neutralize" the metal ion, as suggested for the three nitrogen-containing terpyridines, might relate to the larger size and aliphatic character of the cyclam-ring which supposedly led to a lower partial negative charge at each ring-nitrogen as compared to the pyridine ring. Furthermore, a direct interaction of AspVI:23 in CXCR4 with a cyclam-nitrogen suggests that the chelator itself contributes to the affinity between ligand and receptor. [53]

Future chemokine receptor drugs designed for promiscuity, intrinsic activity and/or allosteric action. The immense role of the chemokine system in inflammatory and allergic diseases has stimulated numerous drug development programs, which so far resulted in two drugs on the market: the CCR5-antagonist Maraviroc which inhibits HIV cell entry, and, as mentioned above, Mozobil (AMD3100), which is used as stemcell mobilizer via CXCR4. This rather low number of successes could arise from the difficulties concerning species differences and the promiscuity of the chemokine system. One way to overcome the latter is to design promiscuous drugs that simultaneously block many chemokine receptors that otherwise could substitute for each other. [46,47]

By analyzing the chelators presented here, similar potency and efficacy-profiles were found for CCR1 and 8 whereas CCR5 was somewhat different (Figure 5), as also confirmed by the focused phylogenetic analysis of residues in the main ligand binding crevice (Figure 3B), and by computational modeling

(Figure 7). Hereby, compounds **11**, **12** and **20** were dual-tropic CCR1 and 8 agonists, while they would discriminate against CCR5. This dual action has been reported previously for the small molecule agonist LMD-559, which is a tetrazole-containing analog of earlier published selective CCR8-agonists, that was found to activate both CCR1 and 8. [43,45] A similar restriction within homologous receptors has also been observed in the MC1 and 4 receptors, where Zn(II) in complex with phenanthroline, 5-methyl- (**11**) or 5-amino-phenanthroline, and bipyridine activated MC1, but not the MC4 receptor despite the presence of a Zn(II)-site in both receptors. [52] In general, dual receptor targeting is suggested as solution to overcome the promiscuity of the chemokine system, and was presented earlier for instance for CCR2 and 5 (TAK-779 and TAK-652 [54,55]), CCR1 and 3 (UCB35625 [56]) CXCR1 and 2 (reparixin [57] and SCH-527123 [58]), but interestingly also for less related receptors such as CCR2 and CXCR2 (thiazolo(4,5-d) pyrimidines [59]) or CCR3 and the histamine H1-receptor (YM-344484 [60]). These examples emphasized the general possibility to find dual ligands also for receptor pairs with low sequence homology, different endogenous ligands and from different receptor subgroups.

Furthermore, most small molecule chemokine ligands are usually allosteric in respect to the endogenous chemokine ligands constituting an extra level of complexity. [4,41,61] It is generally accepted that an allosteric binding-mode provides higher specificity and safety, as the activity depends on the presence of the endogenous ligand, and is limited by the efficacy of this ligand. [62] Interestingly, a study in CCR1 showed that a certain small molecule ligand may act differently on different endogenous ligands (for the same receptor) by being an allosteric enhancer of CCL3 binding, but at the same time competing for CCL5, and by itself acting as agonist for CCR1. [11] A similar phenomenon has been described in CCR5. [39] In the present manuscript a new class of chemokine-receptor ligands, the terpyridines, was identified of

which the chloro-substituted analog (**20**) showed an interesting pharmacological phenomenon, as in this ligand the allosteric enhancing properties were limited to CCR5, while it was a pure agonist on CCR1.

In summary, by studying metal ions in complex with various chelators, it is illustrated how pharmacologic properties can be manipulated. For instance, the ligands potencies could be increased, receptor specificity could be modulated towards only one or two receptors (dual-tropic), and the intrinsic activity could be separated from allosteric properties. The compounds included in the present study are all agonists and/or positive allosteric modulators, however it might be speculated that by finding the right chemical modifications and by substitution of the diffusible metal ion with a covalently linked positively charged group, these compounds could be converted into antagonists of chemokine-action – as supported by the notion that small molecule CC-chemokine receptor antagonists and agonists have similar pharmacophores (centrally located positive charge and flanking aromatic moieties) and exploit the same key-anchor points like GluVII:06/7.39. [44,63,64] Most importantly, the presented metal ion chelators prove that compounds with chemokine- and receptor-dependent allosteric and intrinsic effects can be created and thus illustrate the plurality of actions for small molecules in the chemokine system and the necessity to screen for these various (inter)actions.

EXPERIMENTAL SECTION

Materials. The human chemokines CCL1-3, -5, CCL11-22, -25, CXCL8, -11-13, -16, XCL1 and CX_3CL1 were purchased from Peprotech (NJ, USA). The highest concentration of metal ion chelator complexes ZnBip, ZnPhe, CuBip and CuPhe were made from 0.2 M $ZnCl_2$ in water, 0.2 M $CuSO_4$ in water, 0.4 M phenanthroline in 70% ethanol, 0.4 M bipyridine in DMSO, and were supplemented with 10% DMSO, water and 70% ethanol. Chelator analogs were dissolved in DMSO to 10 mM and prepared in similar ways. Dilutions were made in water. Receptor CCR5 was cloned in house from a leukocyte cDNA library, CCR1-3, CXCR1, -2, -4 and CX_3CR1 cDNA was kindly provided by Tim Wells (GlaxoSmithKline, UK), CXCR3 was kindly provided by Kuldeep Neote (Pfizer), and CCR4, -6-10, CXCR5, -6 and XCR1 were purchased from cDNA.org. The promiscuous G protein $G\alpha_{\Delta 6qi4myr}$ (abbreviated as G_{qi4myr}) was kindly provided by Evi Kostenis (University of Bonn, Germany). *Myo*-[^{3}H]inositol (PT6-271), Bolton-Hunter-Reagent and iodinated chemokine ^{125}I-CCL1 were purchased from PerkinElmer (MA, USA). AG 1-X8 anion exchange resin was from Bio-Rad (CA, USA).

Chemicals and synthetic procedures.

All commercially available starting materials and solvents were used without further purification, unless otherwise stated. THF was freshly distilled from sodium/benzophenone. DMF, Et_3N and TMEDA were dried over 4Å sieves. Purification by flash chromatography was carried out using silica gel 60 (0.040-0.063 mm, Merck). TLC analysis was performed on silica gel 60 F_{254} plates. ^{1}H and ^{13}C NMR spectra were calibrated relative to TMS internal standard or residual solvent peak. High-resolution mass spectra (HRMS) were obtained on Bruker micrOTOF-Q II (ESI) or IonSpec 4.7 T Ultima FTMS using DHB matrix (MALDI). Electron ionization mass spectra were obtained on a Thermo Finnigan SSQ 710 (EI). Purity was determined by HPLC and confirmed by inspection of NMR spectra. HPLC analysis was

performed using a Dionex 120 C18 column (5μ, 4.6x150 mm) with 10% acetonitrile in water (0-1 min), 10-100% acetonitrile in water (1-10 min), 100% acetonitrile (11-15 min), both solvents containing 0.05 % TFA as modifier, a flow of 1 mL/min and UV detection at 230 and 254 nm. All test compounds were of ≥95% purity unless otherwise stated.

6,6'-Dimethyl-2,2'-bipyridine (**1**), 5,5'-dimethyl-2,2'-bipyridine (**2**), 4,4'-dimethyl-2,2'-bipyridine (**3**), 4,4'-dimethoxy-2,2'-bipyridine (**4**), 2,9-dimethyl-1,10-phenanthroline (**5**), 3,4,7,8-tetramethyl-1,10-phenanthroline (**8**), 4-methyl-1,10-phenanthroline (**10**), 5-methyl-1,10-phenanthroline (**11**), 5-chloro-1,10-phenanthroline (**12**), 2,2':6',2''-terpyridine (**18**), 4'-hydroxy-2,2':6',2''-terpyridine (**19**) and 4'-chloro-2,2':6',2''-terpyridine (**20**) were purchased from Sigma-Aldrich. 4,7-Dimethyl-1,10-phenanthroline (**7**) was purchased from Alfa Aesar.

3,8-Dimethyl-1,10-phenanthroline (6). 2-Methylacrylaldehyde (1.4 g, 20 mmol) was added over 5 h to a stirred solution of the *o*-phenylenediamine (650 mg, 6 mmol) and NaI (8.8 mg, 0.0575 mmol) in 70% H_2SO_4 (2.2 mL, 25 mmol) at 110 °C. After 16 h at 110 °C the dark brown reaction mixture was cooled to room temperature, poured into 1 M Na_2CO_3 (25 mL) and extracted with CH_2Cl_2 (3 x 25 mL). The combined organic phases were extracted with 12 M HCl (5 x 10 mL) and the acidic solution is neutralized with 3 M NaOH and 1 M Na_2CO_3 and extracted with CH_2Cl_2 (3 x 50 mL). The combined organic phases were dried ($MgSO_4$), concentrated and a part of the crude product (9.1 mg of 70 mg) was purified by preparative HPLC to give 6 mg of a white solid (89% pure by HPLC).[65] ^{1}H NMR (400 MHz, $CDCl_3$) δ 9.23 (s, 2H), 8.27 (s, 2H), 7.87 (s, 2H), 2.68 (s, 6H); ^{13}C NMR (101 MHz, $CDCl_3$) δ 150.03, 138.37, 134.79, 128.91, 126.91, 19.01; HRMS (ESI) calcd for $C_{14}H_{13}N_2$ ($M + H^+$) 209.1079, found 209.1073.

3-Methyl-1,10-phenanthroline (9). 2-Methylacrylaldehyde (700 mg, 10 mmol) was added over 5 h to a stirred solution of the 8-aminoquinoline (865 mg, 6 mmol) and NaI (8.8 mg, 0.0575 mmol) in 70% H_2SO_4 (2.2 mL, 25 mmol) at 110 °C. After 16 h at 110 °C the dark brown reaction mixture was cooled to

room temperature, poured into 1 M Na_2CO_3 (25 mL) and extracted with CH_2Cl_2 (3 x 25 mL). The combined organic phases were extracted with 12M HCl (5 x 10 mL) and the acidic solution was neutralized with 3M NaOH and 1M Na_2CO_3 and extracted with CH_2Cl_2 (3 x 50 mL). The combined organic phases were dried ($MgSO_4$), concentrated and purified by flash chromatography (SiO_2, CH_2Cl_2) to give 138 mg (12%) of a white solid.[65] R_f = 0.23 (SiO_2, CH_2Cl_2); ^{1}H NMR (400 MHz, $CDCl_3$) δ 9.17 (dd, *J* =4.3, 1.7 Hz, 1H), 9.03 (d, *J* = 2.0 Hz, 1H), 8.22 (dd, *J* = 8.1, 1.7 Hz, 1H), 8.01 (d, *J* = 2.0 Hz, 1H), 7.81–7.68 (m, 2H), 7.60 (dd, *J* = 8.1, 4.3 Hz, 1H), 2.60 (s, 3H); ^{13}C NMR (101 MHz, $CDCl_3$) δ 152.0, 150.4, 146.5, 144.4, 136.0, 135.3, 133.0, 128.5, 128.3, 126.6, 126.4, 122.8, 18.9; HRMS (ESI) calcd for $C_{13}H_{11}N_2$ (M + H^+) 195.0922, found 195.0917.

4,7-Dihydroxy-1,10-phenanthroline (13). The title compound was prepared as described previously.[65]

4,7-Diformyl-1,10-phenanthroline (14). To a solution of 4,7-dimethyl-1,10-phenanthroline (1.093 g, 5.25 mmol) in 1,4-dioxane (100 mL) at room temperature was added selenium dioxide (2.84 g, 25.6 mmol), and the mixture was heated to reflux for two hours. Additional selenium dioxide (3.03 g, 27.3 mmol) was added, and reflux was continued for 16 h. The hot reaction mixture was filtered through a pad of Celite and cooled to room temperature, at which point the product started to precipitate. The solution was put on ice bath to complete the precipitation. The solid was collected and recrystallized from dry THF and dried to provide 530 mg (43%) of the title compound as light orange powder. Rf 0.46 (MeOH with 1% conc. aq. NH_3); ^{1}H NMR in correspondence to previously reported data;[66] ^{13}C NMR (101 MHz, $CDCl_3$) d 194.2, 151.3, 146.0, 136.7, 126.3, 124.6, 123.4; MS (MALDI) 237.1 (M + H^+).

2,9-Bis(hydroxymethyl)-1,10-phenanthroline (15). The title compound was prepared according to a previously described method.[67]

1,10-Phenanthroline-2,9-dicarbaldehyde (16). To a solution of 2,9-dimethyl-1,10-phenanthroline (1.95 g, 9.37 mmol) in 1,4-dioxane (140 mL) was added selenium dioxide (5.25 g, 47.3 mmol) at room

temperature and the reaction mixture was heated to reflux for two hours. The yellow solution changed color via orange and red to green-brown. The warm reaction mixture was filtered to remove a black precipitate and allowed to cool slowly to room temperature. A new precipitate formed, which was filtered off, washed several times with diethyl ether and dried under vacuum to give 1.62 g (73%) of a light grey solid. NMR spectra were in accordance with previously published data.[67]

2,9-Bis(bromomethyl)-1,10-phenanthroline (17). The title compound was prepared according to a previously described method.[67]

Zn(II)-affinity assay: 10 µl of the chelator were added to 90 µl of reaction buffer containing 20 nM ZnCl, 1 µM Fluozin-3 (Invitrogen, UK), 10 mM LiCl in Hank´s balanced salt solution (Invitrogen, UK). After two hours incubation at room temperature, fluorescence intensity (excitation at 485 nm and emission at 520 nm) was measured in a POLARstar Omega from BMG Labtech.

Site-directed Mutagenesis. Point mutations were introduced in the receptors by the polymerase chain reaction overlap extension technique using wt CCR4 and CCR8 as templates. All reactions were carried out using *Pfu* polymerase (Stratagene, CA, USA) under conditions recommended by the manufacturer. The mutations were cloned into the eukaryotic expression vector pcDNA3.1+ and were verified by restriction endonuclease digestion and DNA sequencing (Eurofins MWG Operon, Germany).

Transfections and Tissue Culture. COS-7 cells were grown at 10% CO_2 and 37 °C in Dulbecco´s modified Eagle´s medium with glutamax (Invitrogen, UK) adjusted with 10% fetal bovine serum, 180 units/ml penicillin, and 45 µg/ml penicillin/streptomycin (PenStrep). Transfection of the COS-7 cells was performed by the calcium phosphate precipitation method.[68]

Inositol Phosphate Turnover (IP Turnover). COS-7 cells were transfected according to the procedure mentioned above. Briefly, 6 x 10^6 cells were transfected with 20 µg of receptor cDNA in addition to 30 µg of the promiscuous chimeric G protein, $G\alpha_{qi4myr}$, which turns the $G\alpha_i$-coupled signal, the most common pathway for endogenous chemokine receptors, into the $G\alpha_q$ pathway (phospholipase C activation measured as IP_3 turnover).[68,69] From here two different assays differing in their scale, but which were found to show the same result were carried out. "Traditional" IP_3-assay: One day after transfection, COS-7 cells (1.5 x 10^5 cells/well) were incubated for 24 h with 2 µCi of *myo*[^{3}H]inositol in 0.3 ml of growth medium per well in a 24-well plate. Cells were washed twice in PBS and were incubated in 0.2 ml Hanks´ Balanced Salt Solution (Invitrogen, UK) supplemented with 10 mM LiCl at 37 °C in the presence of various concentrations of ligands. Cells were extracted by addition of 1 ml of 10 mM formic acid to each well followed by incubation on ice for 30 to 60 min. The generated [^{3}H]inositolphosphates were purified on AG 1-X8 anion exchange resin and after addition of Multi Purpose Liquid Scintillation Cocktail (Gold Star, Triskem-International, France), γ-radiation was counted in a Beckman Coulter Counter LS6500. Scintillation proximity assay (SPA)-IP_3: One day after transfection, COS-7 cells (35.000 cells/well) were incubated for 24 h with 0.5 µCi/ml *myo*[^{3}H]inositol in 100 µl of growth medium per well in a 96-well plate. Cells were thereafter treated as mentioned above with volumes adjusted as follows: 100 µl reaction solution with LiCl, 50 µl formic acid. 20µl of the extract were transferred to a white 96-well plate and 80 µl of 1:8 diluted YSi Poly-D-lysine coated beads (Perkin Elmer, MA, USA) were added. Plates were sealed and shaked at maximum speed for at least 30 min, centrifuged for 5 min at 1500 rpm and γ-radiation was counted in a Packard Top Count NXT counter. In both assays, determinations were made in duplicates. This general read-out has previously been used with success in other chemokine receptors.[11,43]

Binding Experiments. 6 x 10^6 COS-7 cells were transfected with 40 μg of receptor cDNA and transferred to culture plates 1 day after transfection. The number of cells seeded per well was determined by the apparent expression efficiency of the receptors and was aimed at obtaining 5-10% specific binding of the added radioactive ligand. Two days after transfection, cells were assayed by competition binding for 3h at 4 °C using 10-15 pM ^{125}I-CCL1 or ^{125}I-CCL3 plus unlabelled ligand in 0.2 ml 50 mM Hepesbuffer pH 7.4, supplemented with 1 mM $CaCl_2$, 5 mM $MgCl_2$, and 0.5% (w/v) bovine serum albumin. After incubation, cells were washed quickly two times in 4 °C binding buffer supplemented with 0.5 M NaCl. Non-specific binding was determined in the presence of 0.1 μM unlabeled CCL1. Determinations were made in duplicates.

Receptor Surface Expression by Enzyme-Linked Immunosorbent Assay (ELISA). COS-7 cells were transiently transfected with the N-terminal FLAG-tagged receptor variants. The cells were washed once in TBS (50 mM Tris-base, 150 mM NaCl, pH 7.6), fixed in 4% glutaraldehyde for 15 min following three washes in TBS and incubation in blocking solution (2% bovine serum albumin in TBS) for 30 min at room temperature. The cells were subsequently incubated two hours with anti-FLAG (M1) antibody (2 μg/ml) (Sigma-Aldrich, MO, USA) in TBS supplemented with 1% bovine serum albumin and 1 mM $CaCl_2$ at room temperature. After three washes in TBS with 1 mM $CaCl_2$, the cells were incubated for 1 h with goat anti-mouse horseradish peroxidase-conjugated antibody (Thermo Fisher Scientific Inc., IL, USA) in the same buffer as the anti-FLAG antibody. After three washes in TBS supplemented with 1 mM $CaCl_2$ the immune reactivity was revealed by the addition of horseradish peroxidase substrate TMB Plus (Kem-En-Tec Diagnostics A/S, Denmark) according to the manufacturer's instruction.

Receptor similarity analysis. Dendograms of all chemokine receptors were produced based on both full-length protein sequences and the residues that could potentially interact with the chelators. The latter were defined as residues with proximity to VII:06/7.39 and side-chains pointing inwards to the trans-membrane cavity and comprised I:03/1.35, I:07/1.39, II:13/2.53, II:20/2.60, III:04/3.28, III:05/3.29, III:08/3.32, III:09/3.33, III:12/3.36, III:13/3.37, V:08/5.42, VI:13/6.48, VI:16/6.51, VI:20/6.55, VII:03/7.36, VII:06/7.39, VII:09/7.42, VII:10/7.43.[70] The alignments were produced with Muscle[71] and manually for the full-length sequences and cavity residues, respectively. Sequence distance matrices were generated using PROTDIST[72] and the default Jones-Taylor-Thornton matrix. Subsequently, unrooted dendograms were calculated with NEIGHBOR[71] and plotted using TreeView.

Molecular Modeling. Models of CCR1, CCR5 and CCR8 were built in two steps. Firstly, halves of the CXCR4 (PDB: 3ODU) helices were superimposed onto agonist-bound/active templates. In this way, the side-chain configurations of the CXCR4 crystal structure were preserved at the same time that the helical backbones were moved to the active conformation. The G protein bound opsin (PDB: 3DQB) was used as the main template, nanobody-stabilized β_2-adrenergic receptor (PDB: 3P0G) was used for the upper parts of TM-5 to 7, and several crystal structures of the Gα C-terminal peptide were superimposed on the one corresponding fragment in the G protein bound opsin structure. From these multiple templates an active CXCR4 model was built using Modeller. Secondly, the CCR1, CCR5 and CCR8 models were built using this CXCR4 models as template.

Calculations. IC_{50} and EC_{50} values were determined by nonlinear regression using the GraphPad-Prism4 software (GraphPad Software, San Diego).

FIGURES

Figure 1. Agonistic activity of the four metal ion chelators ZnBip, ZnPhe, CuBip and CuPhe on all human chemokine receptors (CCR1-10, CXCR1-6, XCR1 and CX_3CR1). The metal ion chelators ZnBip (■), ZnPhe (▲), CuBip (□) and CuPhe (Δ) were tested for their ability to activate chemokine receptors in an assay measuring IP_3 turnover in COS-7 cells co-transfected with receptor and the promiscuous G protein G_{qi4myr}. The curves are normalized to the maximal chemokine induced activation of each receptor, i. e. CCL3 at CCR1, CCL2 on CCR2, CCL11 on CCR3, CCL22 on CCR4, CCL5 on CCR5, CCL20 on CCR6, CCL21 on CCR7, CCL1 on CCR8, CCL25 on CCR9, XCL1 on XCR1, CX3CL1 on CX_3CR1, CXCL8 on CXCR1 and CXCR2, CXCL11 on CXCR3, CXCL12 on CXCR4, CXCL13 on CXCR5 and CXCL16 on CXCR6. For CCR10 no endogenous ligand is available and IP_3-accumulation is therefore shown in cpm/1000 (n = 2-36).

Figure 2. Mutation of GluVII:06/7.39 abrogates metal ion chelator activity. The metal ion chelators CuPhe (Δ), ZnBip, ZnPhe and CuBip (not shown) were tested for their ability to activate mutant receptors [E290A]-CCR4 (A) and [E286A]-CCR8 (B) in an assay as described in the legend to Figure 1. The curves are normalized to the maximal induced activation of CCL1 on [E286A]-CCR8 and CCL22 on CCR4 wt, as for [E290A]-CCR4 no activation by any endogenous chemokine ligand was observed (n=3-5). For comparison, the stippled lines represent activation of wt receptors by CuPhe. A helical wheel diagram of 7TM receptors as seen from the top shows the position of GluVII:06/7.39 in the center of the major binding pocket. Residues highlighted in grey were used for the calculation of a chemogenomic relation of chemokine receptors (Figure 3B) (C).

Figure 3. Phylogenetic and chemogenomic analysis of chemokine receptors. Phylogenetic trees were calculated based on the whole receptor sequence (A) and on residues lining the main ligand binding crevice (highlighted in figure 2C) (B). The former tree represents evolutionary relationships, whereas the latter is enriched for ligand binding (pharmacology) properties. Both trees are neighbor-joining trees generated with Phylip and branch lengths correspond to sequence similarities.

Figure 4. The chelators affinities for Zn(II). The chelators affinity for Zn(II)-ions was determined in a fluorescence based assay using the Zn(II)-sensitive fluorophore FluoZin3 (n = 3-4). The affinity is given as pIC_{50} and chelators are sorted from lowest (left) to highest (right) Zn(II)-affinity. Chelators with bi-pyridine-scaffolds are highlighted in dark grey, phenanthroline-scaffolds in light grey and terpyridine-scaffolds in white. Underneath the diagram, the substituents and their positions are indicated with m^1, p^1 meaning mono-substitution and o^2, m^2, p^2 meaning di-substitution in *ortho*-, *meta*- and *para*-position, respectively, and "central" referring to the 4'-position in 2,2':6',2''-terpyridines.

Figure 5. Zn(II)-affinities and potencies of the chelators in complex with Zn(II) are positively correlated. The Zn(II)-affinities (stippled line) and potencies of Zn(II)-chelator complexes at CCR1 (□), CCR8 (○) and CCR5 (▲) are given, sorted from the lowest to highest CCR1-potency. For simplification, chelators that showed no activation are referred to as having a pEC_{50} = 3 (compare with Table 1) (A). In (B) the efficacies as fold above basal are given on CCR1, CCR8 and CCR5 using the same symbols and order (n = 3-39). The number of the compound, its scaffold, position of substitution and substituent are given underneath the diagrams using the same nomenclature as in Figure 4.

Figure 6. CCR1 and CCR8 are similar, but different from CCR5. The ability of chelator analogs 4,4'-dimethyl-2,2'-bipyridine (**3**, □), 5,5'-dimethyl-2,2'-bipyridine (**2**, ■) (A-C), 5-methyl-1,10-phenanthroline (**11**, ▲), 5-chloro-1,10-phenanthroline (**12**, Δ) (D-F) and 2,2':6',2''-terpyridine (**18**, ○), 4'-chloro-2,2':6',2''-terpyridine (**20**, ●) (G-I) to activate CCR1 (A, D, G), CCR8 (B, E, H) and CCR5 (C, F, I), as determined in an IP_3-turnover assay as described in the legend to Figure 1, is shown (n = 3-8). For comparison activation by the relative control-compounds ZnBip (A-C, G-I) or ZnPhe (D-F) is presented as stippled lines (n = 20-39). The structures of the chelators are given on the right side.

Figure 7. Models of receptors CCR1, CCR8 and CCR5 emphasize structural differences of these receptors. A representation of the CCR1-model as seen from the membrane (A) indicates the position of GluVII:06/7.39 and the approximate depth of presentations in B, C and D, where the main ligand binding crevices of CCR1 (B), CCR8 (C) and CCR5 (D) are shown from the top using models of each receptor in its proposed active conformation. The pocket area was created with negative charges in red, positive charges in blue, and sulfurs in yellow. Only the inside of the pockets surface areas was illuminated so that their outside appears black, giving a better impression of their 3-dimensional structure. Green arrows and circles in D highlight the special features that differ tremendously between CCR1/8 and CCR5. As indicated in the text, these differences comprise a deeper major binding pocket in CCR5, that also extents towards TM-4/5. The minor binding pocket is shallower in CCR5, and narrower in the area around TM-2, but protrudes further between TM-1 and -7 as compared to in CCR1 and CCR8.

Figure 8. Test of the new class of 2,2':6',2''-terpyridines in binding of ^{125}I-CCL3 to CCR1 and CCR5. The effect of **18** (○), **20** (●) and Bip (stippled line) in complex with Zn(II) on the binding of ^{125}I-CCL3 to

CCR1 (A) or CCR5 (B) was measured by heterologous competition binding experiments in COS-7 cells transfected with receptor. The curves are normalized to specifically bound ^{125}I-CCL3 in the absence of cold ligand (n = 4-5).

CHARTS

Chart 1. Structures of the chelator analogs. The structure of chelators sorted by lead-structure are given: 2,2'-bipyridines (A), 1,10-phenanthrolines (B) and 2,2':6',2''-terpyridines (C). The *ortho*-, *meta*-, and *para*-positions in 2,2'-bipyridine and 1,10-phenanthroline are indicated by *o, o', m, m'* and *p, p'*, respectively.

TABLES

Table 1. The chelators affinity to Zn(II) and their potency at activating CCR1, CCR8 and CCR5. The chelator structures are presented in Chart 1. Their basic scaffold, position of substitution (Pos.), substituent (Subst.) and full name are given in the left of the table. The affinity of the chelators to Zn(II) was assessed in a fluorescence based assays with the Zn(II)-sensitive fluorophore FluoZin3. IP_3 turnover was measured in COS-7 cells co-transfected with receptor and chimeric G protein G_{qi4myr}, as described in the legend to Figure 1. The EC_{50} values are given in log and μM. F_{lig} indicates the fold-increase of potency for a Zn(II)-chelator-complex as compared to either ZnBip (for Bip-analogs and terpyridines) or ZnPhe (for Phe-analogs) on the respective receptor. A fold-increase > 2 is highlighted in light green, > 5 medium green and > 10 dark green. The efficacies are given as fold over basal and the number of experiments (n) is shown in parentheses. An asterisk indicates a biphasic shape of the curve, where only the activating potency is given, while the ligand showed antagonistic activity at higher concentrations. Due to the diffi-

culty of interpreting this observation, this compound (**5**) is depicted as "inactive" with a pEC_{50} = 3, and efficacies with a fold-above basal = 1 in Figure 5.

Table 2. Test of the chelator analogs in complex with Zn(II) in competition binding experiments of ^{125}I-CCL3 to CCR1 and CCR5. The effect of Zn(II)-chelator complexes on the binding of ^{125}I-CCL3 to CCR1 and CCR5 was tested in a heterologous competition binding experiment. The affinity is given as IC_{50} in log ± SEM and μM, and the maximal enhanced binding (in %) above specifically bound ^{125}I-CCL3 in the absence of cold ligand (set as 100%) are given. The number of experiments (n) is given.

ASSOCIATED CONTENT

Supporting Information. There are additional data for control experiments, competition binding of ^{125}I-CCL3 to wt CCR1 and wt CCR5, ^{125}I-CCL1 binding to wt CCR8, activation by endogenous ligands and surface expression of [E290A]-CCR4 and [E286A]-CCR8 as well as graphs displaying the relationship between chelator-Zn(II)-affinity and potency at CCR1, 5 and 8. This material is available free of charge via the Internet at http://pubs.acs.org.

AUTHOR INFORMATION

Corresponding Author

* Corresponding author: Mette M. Rosenkilde; telephone: 0045 30604608, email: rosenkilde@sund.ku.dk

Present Addresses

† Mads C. Nielsen, Swiss Federal Institute of Technology Zurich, Department of Chemistry and Applied Biosciences, Wolfgang-Pauli-Str. 10, Ch-8093 Zurich, Switzerland

† Mikkel Malmgaard-Clausen, Xellia Pharmaceuticals ApS, Dahlslandsgade 11, Dk-2300 Copenhagen, Denmark

ACKNOWLEDGMENT

The authors would like to thank Randi Thøgersen for excellent technical assistance. The studies were supported by The Danish Council for Independent Research | Medical Sciences, the NovoNordisk Foundation, the Lundbeck Foundation, the European Community´s Sixth Framework program (INNOCHEM: LSHB-CT-2005-518167), the AP-Moller Foundation and the Aase and Einar Danielsen Foundation. The authors declare no competing financial interest.

ABBREVIATIONS

7TM, 7 transmembrane; Bip, bipyridine; CCL, CC-chemokine ligand; CCR, CC-chemokine receptor; CX_3CL, CX_3C-chemokine ligand; CX_3CR, CX_3C-chemokine receptor; CXCL, CXC-chemokine ligand; CXCR, CXC-chemokine receptor; GPCR, G protein-coupled receptor; HHV8, human Herpesvirus 8; HIV, human immunodeficiency virus; MC1 and MC4, melanocortin 1 and 4; NK1, neurokinin or tachykinin or substance P; NK2, neurokinin 2 or tachykinin 2; NK3, neurokinin 3 or neurokinin B; ORF, open reading frame; Phe, phenanthroline; TM, transmembrane helix; wt, wildtype; XCL, XC-chemokine ligand; XCR, XC-chemokine receptor

REFERENCES

(1) Vassilatis, D. K.; Hohmann, J. G.; Zeng, H.; Li, F.; Ranchalis, J. E.; Mortrud, M. T.; Brown, A.; Rodriguez, S. S.; Weller, J. R.; Wright, A. C.; Bergmann, J. E.; Gaitanaris, G. A. The G protein-coupled receptor repertoires of human and mouse. *Proc. Natl. Acad. Sci. U. S. A.* **2003**, *100*, 4903-4908.

(2) Overington, J. P.; Al-Lazikani, B.; Hopkins, A. L. How many drug targets are there? *Nat. Rev. Drug. Discov.* **2006**, *5*, 993-996.

(3) Viola, A.; Luster, A. D. Chemokines and their receptors: drug targets in immunity and inflammation. *Annu. Rev. Pharmacol. Toxicol.* **2008**, *48*, 171-197.

(4) Scholten, D.; Canals, M.; Maussang, D.; Roumen, L.; Smit, M.; Wijtmans, M.; de Graaf, C.; Vischer, H.; Leurs, R. Pharmacological Modulation of Chemokine Receptor Function. *Br. J. Pharmacol.* **2012**, *165*, 1617-1643.

(5) Mantovani, A. The chemokine system: redundancy for robust outputs. *Immunol. Today.* **1999**, *20*, 254-257.

(6) Murphy, P. M.; Baggiolini, M.; Charo, I. F.; Hébert, C. A.; Horuk, R.; Matsushima, K.; Miller, L. H.; Oppenheim, J. J.; Power, C. A. International union of pharmacology. XXII. Nomenclature for chemokine receptors. *Pharmacol. Rev.* **2000**, *52*, 145-176.

(7) Allen, S. J.; Crown, S. E.; Handel, T. M. Chemokine: receptor structure, interactions, and antagonism. *Annu. Rev. Immunol.* **2007**, *25*, 787-820.

(8) Proudfoot, A. E.; Power, C. A.; Schwarz, M. K. Anti-chemokine small molecule drugs: a promising future? *Expert. Opin. Investig. Drugs.* **2010**, *19*, 345-355.

(9) Monteclaro, F. S.; Charo, I. F. The amino-terminal extracellular domain of the MCP-1 receptor, but not the RANTES/MIP-1alpha receptor, confers chemokine selectivity. Evidence for a two-step mechanism for MCP-1 receptor activation. *J. Biol. Chem.* **1996**, *271*, 19084-19092.

(10) Blanpain, C.; Doranz, B. J.; Bondue, A.; Govaerts, C.; De Leener, A.; Vassart, G.; Doms, R. W.; Proudfoot, A.; Parmentier, M. The core domain of chemokines binds CCR5 extracellular domains while their amino terminus interacts with the transmembrane helix bundle. *J. Biol. Chem.* **2003**, *278*, 5179-5187.

(11) Jensen, P. C.; Thiele, S.; Ulven, T.; Schwartz, T. W.; Rosenkilde, M. M. Positive versus negative modulation of different endogenous chemokines for CC-chemokine receptor 1 by small molecule agonists through allosteric versus orthosteric binding. *J. Biol. Chem.* **2008**, *283*, 23121-23128.

(12) Footnote

(13) Oteiza, P. I.; Mackenzie, G. G. Zinc, oxidant-triggered cell signaling, and human health. *Mol. Aspects. Med.* **2005**, *26*, 245-255.

(14) Norregaard, L.; Frederiksen, D.; Nielsen, E. O.; Gether, U. Delineation of an endogenous zinc-binding site in the human dopamine transporter. *EMBO. J.* **1998**, *17*, 4266-4273.

(15) Rosenkilde, M. M.; Lucibello, M.; Holst, B.; Schwartz, T. W. Natural agonist enhancing bis-His zinc-site in transmembrane segment V of the tachykinin NK3 receptor. *FEBS. Lett.* **1998**, *439*, 35-40.

(16) Hsiao, B.; Dweck, D.; Luetje, C. W. Subunit-dependent modulation of neuronal nicotinic receptors by zinc. *J. Neurosci.* **2001**, *21*, 1848-1856.

(17) Takeda, A.; Minami, A.; Seki, Y.; Oku, N. Differential effects of zinc on glutamatergic and GABAergic neurotransmitter systems in the hippocampus. *J. Neurosci. Res.* **2004**, *75*, 225-229.

(18) Schwartz, T. W.; Frimurer, T. M.; Holst, B.; Rosenkilde, M. M.; Elling, C. E. Molecular mechanism of 7TM receptor activation--a global toggle switch model. *Annu. Rev. Pharmacol. Toxicol.* **2006**, *46*, 481-519.

(19) Elling, C. E.; Frimurer, T. M.; Gerlach, L. O.; Jorgensen, R.; Holst, B.; Schwartz, T. W. Metal ion site engineering indicates a global toggle switch model for seven-transmembrane receptor activation. *J. Biol. Chem.* **2006**, *281*, 17337-17346.

(20) Rosenkilde, M. M.; Andersen, M. B.; Nygaard, R.; Frimurer, T. M.; Schwartz, T. W. Activation of the CXCR3 chemokine receptor through anchoring of a small molecule chelator ligand between TM-III, -IV, and -VI. *Mol. Pharmacol.* **2007**, *71*, 930-941.

(21) Hubbell, W. L.; Altenbach, C.; Hubbell, C. M.; Khorana, H. G. Rhodopsin structure, dynamics, and activation: a perspective from crystallography, site-directed spin labeling, sulfhydryl reactivity, and disulfide cross-linking. *Adv. Protein. Chem.* **2003**, *63*, 243-290.

(22) Altenbach, C.; Kusnetzow, A. K.; Ernst, O. P.; Hofmann, K. P.; Hubbell, W. L. High-resolution distance mapping in rhodopsin reveals the pattern of helix movement due to activation. *Proc. Natl. Acad. Sci. U. S. A.* **2008**, *105*, 7439-7444.

(23) Park, J. H.; Scheerer, P.; Hofmann, K. P.; Choe, H. W.; Ernst, O. P. Crystal structure of the ligand-free G-protein-coupled receptor opsin. *Nature.* **2008**, *454*, 183-187.

(24) Scheerer, P.; Park, J. H.; Hildebrand, P. W.; Kim, Y. J.; Krauss, N.; Choe, H. W.; Hofmann, K. P.; Ernst, O. P. Crystal structure of opsin in its G-protein-interacting conformation. *Nature.* **2008**, *455*, 497-502.

(25) Rasmussen, S. G.; Choi, H. J.; Fung, J. J.; Pardon, E.; Casarosa, P.; Chae, P. S.; Devree, B. T.; Rosenbaum, D. M.; Thian, F. S.; Kobilka, T. S.; Schnapp, A.; Konetzki, I.; Sunahara, R. K.; Gellman, S. H.; Pautsch, A.; Steyaert, J.; Weis, W. I.; Kobilka, B. K. Structure of a nanobody-stabilized active state of the β(2) adrenoceptor. *Nature.* **2011**, *469*, 175-180.

(26) Rasmussen, S. G.; DeVree, B. T.; Zou, Y.; Kruse, A. C.; Chung, K. Y.; Kobilka, T. S.; Thian, F. S.; Chae, P. S.; Pardon, E.; Calinski, D.; Mathiesen, J. M.; Shah, S. T.; Lyons, J. A.; Caffrey, M.; Gellman, S.

H.; Steyaert, J.; Skiniotis, G.; Weis, W. I.; Sunahara, R. K.; Kobilka, B. K. Crystal structure of the β2 adrenergic receptor-Gs protein complex. *Nature.* **2011**, *477*, 549-555.

(27) Elling, C. E.; Nielsen, S. M.; Schwartz, T. W. Conversion of antagonist-binding site to metal-ion site in the tachykinin NK-1 receptor. *Nature.* **1995**, *374*, 74-77.

(28) Thirstrup, K.; Elling, C. E.; Hjorth, S. A.; Schwartz, T. W. Construction of a high affinity zinc switch in the kappa-opioid receptor. *J. Biol. Chem.* **1996**, *271*, 7875-7878.

(29) Rosenkilde, M. M.; Kledal, T. N.; Bräuner-Osborne, H.; Schwartz, T. W. Agonists and inverse agonists for the herpesvirus 8-encoded constitutively active seven-transmembrane oncogene product, ORF-74. *J. Biol. Chem.* **1999**, *274*, 956-961.

(30) Holst, B.; Elling, C. E.; Schwartz, T. W. Partial agonism through a zinc-Ion switch constructed between transmembrane domains III and VII in the tachykinin NK(1) receptor. *Mol. Pharmacol.* **2000**, *58*, 263-270.

(31) Jensen, A. A.; Sheppard, P. O.; Jensen, L. B.; O'Hara, P. J.; Bräuner-Osborne, H. Construction of a high affinity zinc binding site in the metabotropic glutamate receptor mGluR1: noncompetitive antagonism originating from the amino-terminal domain of a family C G-protein-coupled receptor. *J. Biol. Chem.* **2001**, *276*, 10110-10118.

(32) Swaminath, G.; Lee, T. W.; Kobilka, B. Identification of an allosteric binding site for Zn2+ on the beta2 adrenergic receptor. *J. Biol. Chem.* **2003**, *278*, 352-356.

(33) Rosenkilde, M. M.; David, R.; Oerlecke, I.; Benned-Jensen, T.; Geumann, U.; Beck-Sickinger, A. G.; Schwartz, T. W. Conformational constraining of inactive and active States of a seven transmembrane receptor by metal ion site engineering in the extracellular end of transmembrane segment V. *Mol. Pharmacol.* **2006**, *70*, 1892-1901.

(34) Storjohann, L.; Holst, B.; Schwartz, T. W. Molecular mechanism of Zn2+ agonism in the extracellular domain of GPR39. *FEBS. Lett.* **2008**, *582*, 2583-2588.

(35) Footnote

(36) Schwartz, T. W. Locating ligand-binding sites in 7TM receptors by protein engineering. *Curr. Opin. Biotechnol.* **1994**, *5*, 434-444.

(37) Baldwin, J. M.; Schertler, G. F.; Unger, V. M. An alpha-carbon template for the transmembrane helices in the rhodopsin family of G-protein-coupled receptors. *J. Mol. Biol.* **1997**, *272*, 144-164.

(38) Ballesteros, J.A.; Weinstein, H. Integrated methods for the construction of three-dimensional models and computational probing of structure-function relations in G protein-coupled receptors. *Receptor Molecular Biology*; Sealfon S. C., ed.; 1995 pp 366-428.

(39) Thiele, S.; Steen, A.; Jensen, P. C.; Mokrosinski, J.; Frimurer, T. M.; Rosenkilde, M. M. Allosteric and orthosteric sites in CC chemokine receptor (CCR5), a chimeric receptor approach. *J. Biol. Chem.* **2011**, *286*, 37543-37554.

(40) Rosenkilde, M. M.; Benned-Jensen, T.; Frimurer, T. M.; Schwartz, T. W. The minor binding pocket: a major player in 7TM receptor activation. *Trends. Pharmacol. Sci.* **2010**, *31*, 567-574.

(41) Rosenkilde, M. M.; Schwartz, T. W. GluVII:06--a highly conserved and selective anchor point for non-peptide ligands in chemokine receptors. *Curr. Top. Med. Chem.* **2006**, *6*, 1319-1333.

(42) Hemmerich, S.; Paavola, C.; Bloom, A.; Bhakta, S.; Freedman, R.; Grunberger, D.; Krstenansky, J.; Lee, S.; McCarley, D.; Mulkins, M.; Wong, B.; Pease, J.; Mizoue, L.; Mirzadegan, T.; Polsky, I.; Thompson, K.; Handel, T. M.; Jarnagin, K. Identification of residues in the monocyte chemotactic protein-1 that contact the MCP-1 receptor, CCR2. *Biochemistry.* **1999**, *38*, 13013-13025.

(43) Jensen, P. C.; Nygaard, R.; Thiele, S.; Elder, A.; Zhu, G.; Kolbeck, R.; Ghosh, S.; Schwartz, T. W.; Rosenkilde, M. M. Molecular interaction of a potent nonpeptide agonist with the chemokine receptor CCR8. *Mol. Pharmacol.* **2007**, *72*, 327-340.

(44) Jensen, P. C.; Thiele, S.; Steen, A.; Elder, A.; Kolbeck, R.; Ghosh, S.; Frimurer, T. M.; Rosenkilde, M. M. Reversed binding of a small molecles ligand in homologous chemokine receptors - differential role of extracellular loop 2. *Br. J. Pharmacol.* **2012**, *166*, 258-275.

(45) Sierro, F.; Biben, C.; Martínez-Muñoz, L.; Mellado, M.; Ransohoff, R. M.; Li, M.; Woehl, B.; Leung, H.; Groom, J.; Batten, M.; Harvey, R. P.; Martínez-A, C.; Mackay, C. R.; Mackay, F. Disrupted cardiac development but normal hematopoiesis in mice deficient in the second CXCL12/SDF-1 receptor, CXCR7. *Proc. Natl. Acad. Sci. U. S. A.* **2007**, *104*, 14759-14764.

(46) Horuk, R. Promiscuous drugs as therapeutics for chemokine receptors. *Expert. Rev. Mol. Med.* **2009**, *11*, e1.

(47) Pease, J. E.; Horuk, R. Small molecule antagonists of chemokine receptors--is promiscuity a virtue? *Curr. Top. Med. Chem.* **2010**, *10*, 1351-1358.

(48) Footnote

(49) Clavier, S.; Rist, O.; Hansen, S.; Gerlach, L. O.; Högberg, T.; Bergman, J. Preparation and evaluation of sulfur-containing metal chelators. *Org. Biomol. Chem.* **2003**, *1*, 4248-4253.

(50) Wu, B.; Chien, E. Y.; Mol, C. D.; Fenalti, G.; Liu, W.; Katritch, V.; Abagyan, R.; Brooun, A.; Wells, P.; Bi, F. C.; Hamel, D. J.; Kuhn, P.; Handel, T. M.; Cherezov, V.; Stevens, R. C. Structures of the CXCR4 chemokine GPCR with small-molecule and cyclic peptide antagonists. *Science.* **2010**, *330*, 1066-1071.

(51) Elling, C. E.; Thirstrup, K.; Holst, B.; Schwartz, T. W. Conversion of agonist site to metal-ion chelator site in the beta(2)-adrenergic receptor. *Proc. Natl. Acad. Sci. U. S. A.* **1999**, *96*, 12322-12327.

(52) Holst, B.; Elling, C. E.; Schwartz, T. W. Metal ion-mediated agonism and agonist enhancement in melanocortin MC1 and MC4 receptors. *J. Biol. Chem.* **2002**, *277*, 47662-47670.

(53) Gerlach, L. O.; Jakobsen, J. S.; Jensen, K. P.; Rosenkilde, M. R.; Skerlj, R. T.; Ryde, U.; Bridger, G. J.; Schwartz, T. W. Metal ion enhanced binding of AMD3100 to Asp262 in the CXCR4 receptor. *Biochemistry.* **2003**, *42*, 710-717.

(54) Baba, M.; Nishimura, O.; Kanzaki, N.; Okamoto, M.; Sawada, H.; Iizawa, Y.; Shiraishi, M.; Aramaki, Y.; Okonogi, K.; Ogawa, Y.; Meguro, K.; Fujino, M. A small-molecule, nonpeptide CCR5 antagonist with highly potent and selective anti-HIV-1 activity. *Proc. Natl. Acad. Sci. U. S. A.* **1999**, *96*, 5698-5703.

(55) Seto, M.; Aikawa, K.; Miyamoto, N.; Aramaki, Y.; Kanzaki, N.; Takashima, K.; Kuze, Y.; Iizawa, Y.; Baba, M.; Shiraishi, M. Highly potent and orally active CCR5 antagonists as anti-HIV-1 agents: synthesis and biological activities of 1-benzazocine derivatives containing a sulfoxide moiety. *J. Med. Chem.* **2006**, *49*, 2037-2048.

(56) Sabroe, I.; Peck, M. J.; Van Keulen, B. J.; Jorritsma, A.; Simmons, G.; Clapham, P. R.; Williams, T. J.; Pease, J. E. A small molecule antagonist of chemokine receptors CCR1 and CCR3. Potent inhibition of eosinophil function and CCR3-mediated HIV-1 entry. *J. Biol. Chem.* **2000**, *275*, 25985-25992.

(57) Allegretti, M.; Bertini, R.; Cesta, M. C.; Bizzarri, C.; Di Bitondo, R.; Di Cioccio, V.; Galliera, E.; Berdini, V.; Topai, A.; Zampella, G.; Russo, V.; Di Bello, N.; Nano, G.; Nicolini, L.; Locati, M.; Fantucci, P.; Florio, S.; Colotta, F. 2-Arylpropionic CXC chemokine receptor 1 (CXCR1) ligands as novel noncompetitive CXCL8 inhibitors. *J. Med. Chem.* **2005**, *48*, 4312-4331.

(58) Dwyer, M. P.; Yu, Y.; Chao, J.; Aki, C.; Chao, J.; Biju, P.; Girijavallabhan, V.; Rindgen, D.; Bond, R.; Mayer-Ezel, R.; Jakway, J.; Hipkin, R. W.; Fossetta, J.; Gonsiorek, W.; Bian, H.; Fan, X.; Terminelli, C.; Fine, J.; Lundell, D.; Merritt, J. R.; Rokosz, L. L.; Kaiser, B.; Li, G.; Wang, W.; Stauffer, T.; Ozgur, L.;

Baldwin, J.; Taveras, A. G. Discovery of 2-hydroxy-N,N-dimethyl-3-{2-[[(R)-1-(5- methylfuran-2-yl)propyl]amino]-3,4-dioxocyclobut-1-enylamino}benzamide (SCH 527123): a potent, orally bioavailable CXCR2/CXCR1 receptor antagonist. *J. Med. Chem.* **2006**, *49*, 7603-7606.

(59) Walters, I.; Austin, C.; Austin, R.; Bonnert, R.; Cage, P.; Christie, M.; Ebden, M.; Gardiner, S.; Grahames, C.; Hill, S.; Hunt, F.; Jewell, R.; Lewis, S.; Martin, I.; David Nicholls; David Robinson Evaluation of a series of bicyclic CXCR2 antagonists. *Bioorg. Med. Chem. Lett.* **2008**, *18*, 798-803.

(60) Suzuki, K.; Morokata, T.; Morihira, K.; Sato, I.; Takizawa, S.; Kaneko, M.; Takahashi, K.; Shimizu, Y. A dual antagonist for chemokine CCR3 receptor and histamine H1 receptor. *Eur. J. Pharmacol.* **2007**, *563*, 224-232.

(61) Steen, A.; Schwartz, T. W.; Rosenkilde, M. M. Targeting CXCR4 in HIV Cell-Entry Inhibition. *Mini. Rev. Med. Chem.* **2010**, *17*, 1605-1621.

(62) May, L. T.; Leach, K.; Sexton, P. M.; Christopoulos, A. Allosteric modulation of G protein-coupled receptors. *Annu. Rev. Pharmacol. Toxicol.* **2007**, *47*, 1-51.

(63) Schwartz, T. W.; Rosenkilde, M. M. Is there a 'lock' for all agonist 'keys' in 7TM receptors? *Trends. Pharmacol. Sci.* **1996**, *17*, 213-216.

(64) Jensen, P. C.; Rosenkilde, M. M. Chapter 8. Activation mechanisms of chemokine receptors. *Methods. Enzymol.* **2009**, *461*, 171-190.

(65) Altman, R. A.; Buchwald, S. L. 4,7-Dimethoxy-1,10-phenanthroline: an excellent ligand for the Cu-catalyzed N-arylation of imidazoles. *Org. Lett.* **2006**, *8*, 2779-2782.

(66) Lin, H.; Yu, X.; Lin, H. K. A colorimetric anion receptor containing the cis-Ru(bipy)(2)(2+)group. *Trans. Met. Chem.* **2008**, *33*, 829-834.

(67) Chandler, C. J.; Deady, L. W.; Reiss Synthesis of some 2,9-disubstituted-1,10-phenanthrolines. *J. Heterocycl. Chem.* **1981**, *18*, 599-602.

(68) Rosenkilde, M. M.; Cahir, M.; Gether, U.; Hjorth, S. A.; Schwartz, T. W. Mutations along transmembrane segment II of the NK-1 receptor affect substance P competition with non-peptide antagonists but not substance P binding. *J. Biol. Chem.* **1994**, *269*, 28160-28164.

(69) Kostenis, E.; Zeng, F. Y.; Wess, J. Functional characterization of a series of mutant G protein alphaq subunits displaying promiscuous receptor coupling properties. *J. Biol. Chem.* **1998**, *273*, 17886-17892.

(70) Gloriam, D. E.; Foord, S. M.; Blaney, F. E.; Garland, S. L. Definition of the G protein-coupled receptor transmembrane bundle binding pocket and calculation of receptor similarities for drug design. *J. Med. Chem.* **2009**, *52*, 4429-4442.

(71) Edgar, R. C. MUSCLE: multiple sequence alignment with high accuracy and high throughput. *Nucleic. Acids. Res.* **2004**, *32*, 1792-1797.

(72) Felsenstein, J. PHYLIP (Phylogeny Inference Package) version 3.6. *Distributed. by. the. author.* **2008**.

FOOTNOTES

(12) The systematic nomenclature for chemokines after Murphy *et al.* is used throughout the article.[6]

(35) The generic numbering systems suggested by Baldwin and Schwartz[36,37] is used throughout the manuscript followed by the Ballesteros/Weinstein numbering system.[38]

(48) A similar test could not be performed for CCR4, as the radiolabeled versions of the two endogenous CCR4 ligands CCL22 and CCL17 are not commercially available.

Table of Contents graphic

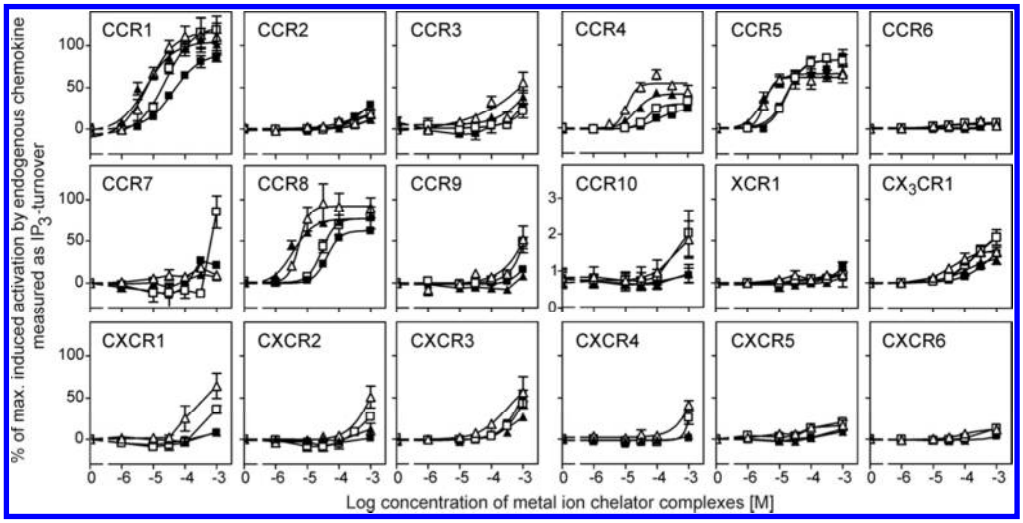

Agonistic activity of the four metal ion chelators ZnBip, ZnPhe, CuBip and CuPhe on all human chemokine receptors (CCR1-10, CXCR1-6, XCR1 and CX3CR1).
88x44mm (300 x 300 DPI)

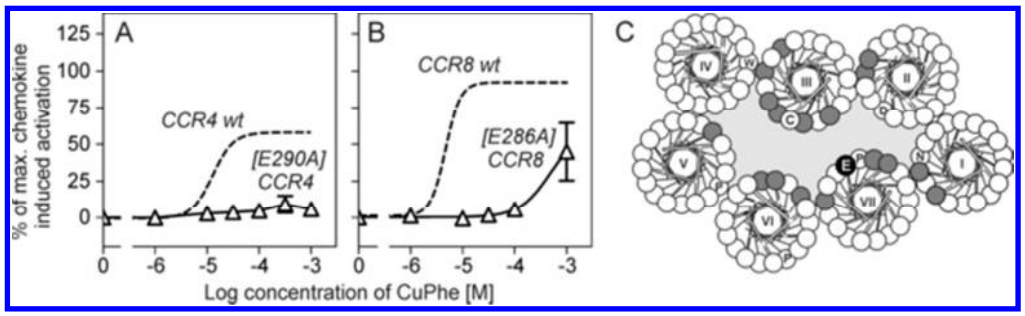

Mutation of GluVII:06/7.39 abrogates metal ion chelator activity.
51x14mm (300 x 300 DPI)

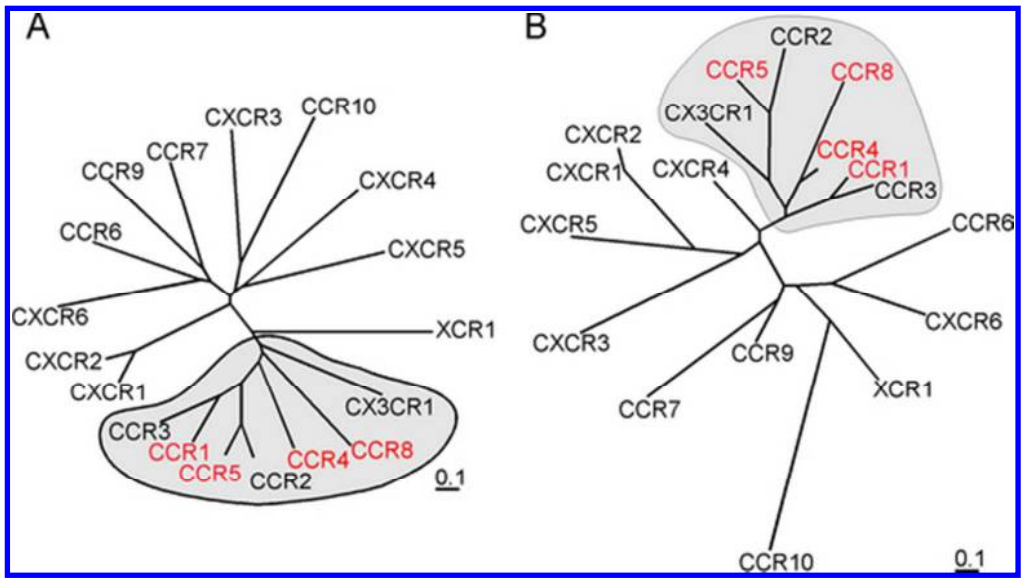

Phylogenetic and chemogenomic analysis of chemokine receptors.
47x26mm (300 x 300 DPI)

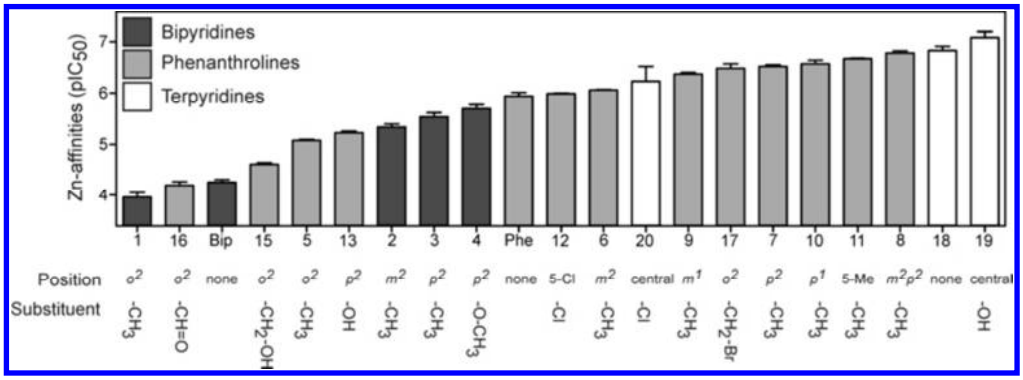

The chelators affinities for Zn(II).
63x22mm (300 x 300 DPI)

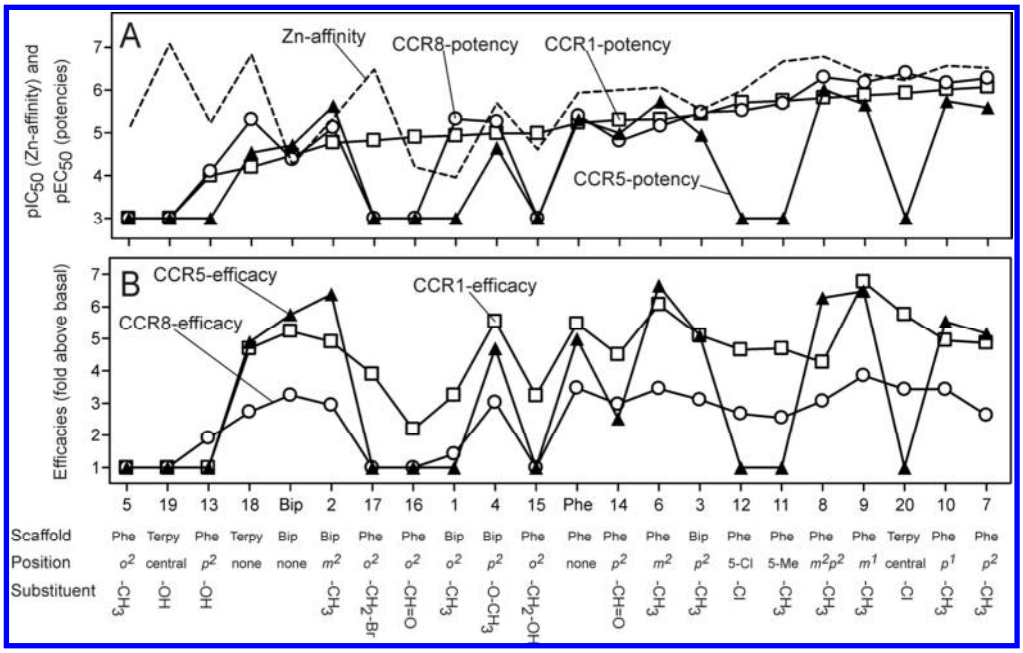

Zn(II)-affinities and potencies of the chelators n complex with Zn(II) are positively correlated.
112x70mm (300 x 300 DPI)

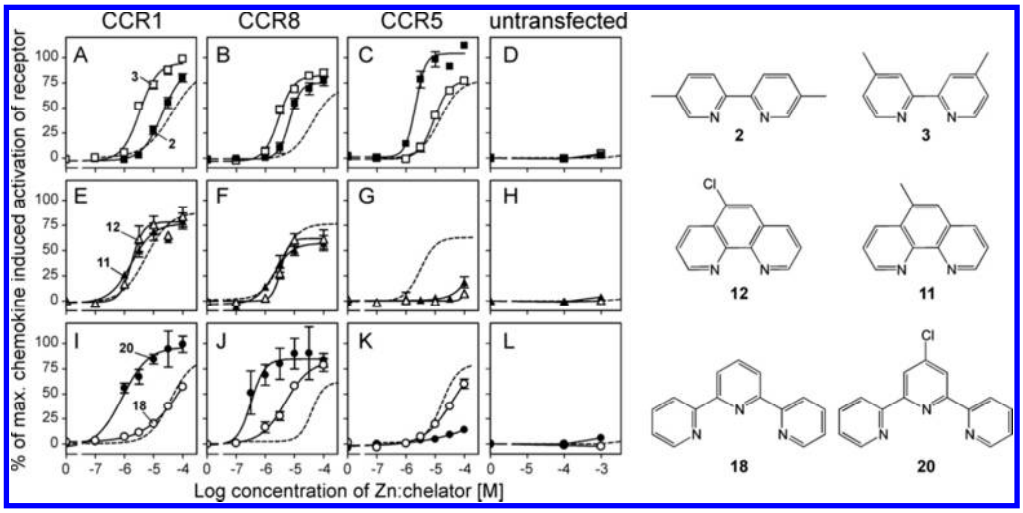

87x42mm (300 x 300 DPI)

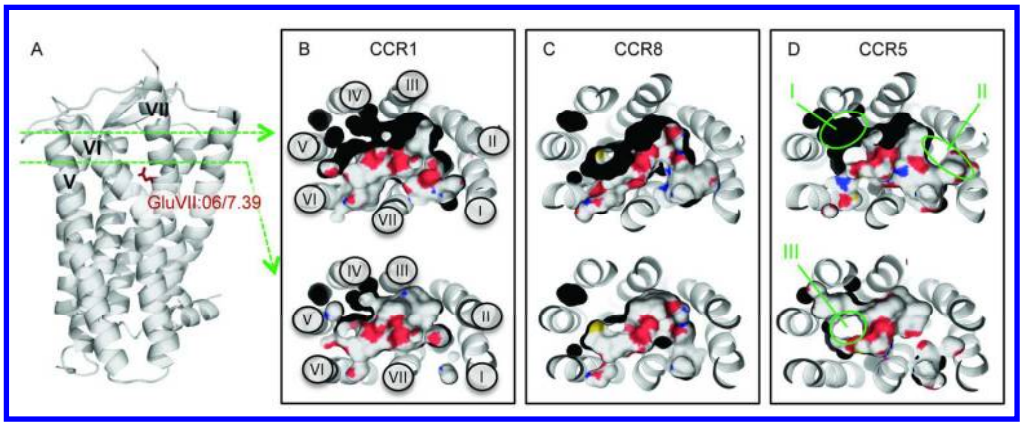

Models of receptors CCR1, CCR8 and CCR5 emphasize structural differences of these receptors.
71x28mm (600 x 600 DPI)

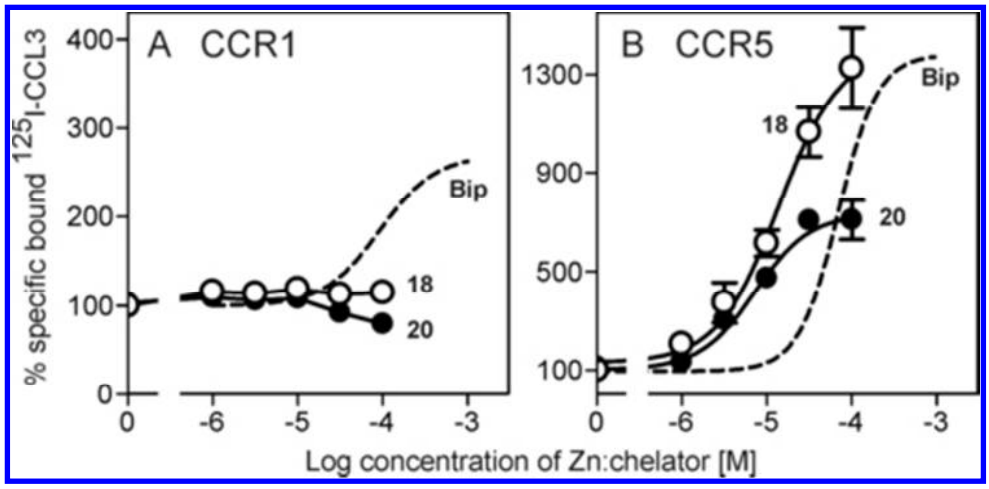

Test of the new class of 2,2'-6',2''-terpyridines in binding of 125I-CCL3 to CCR1 and CCR5.
40x19mm (300 x 300 DPI)

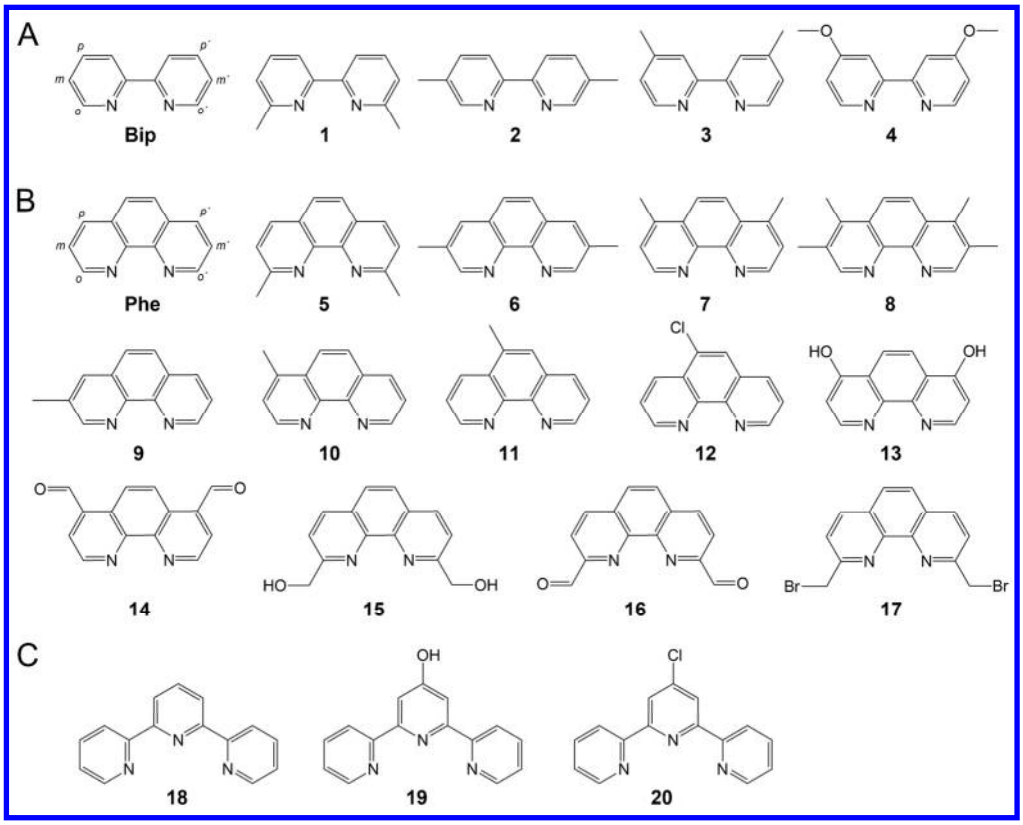

Structures of the chelator analogs.
142x114mm (300 x 300 DPI)

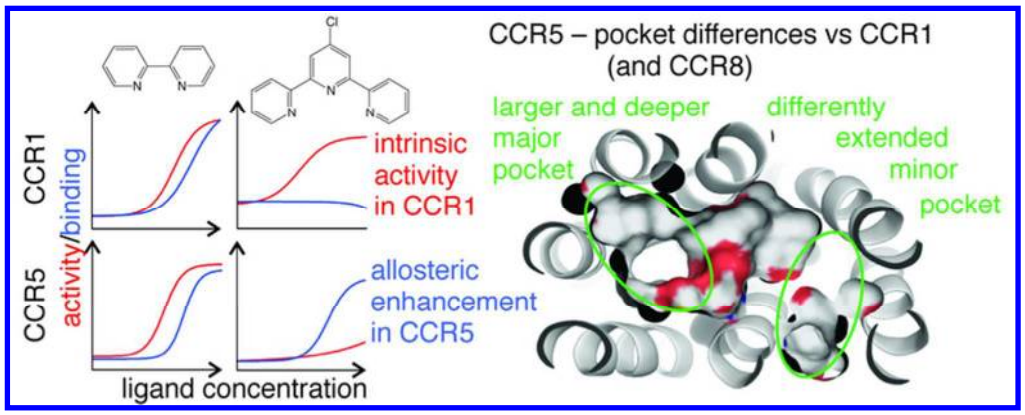

Synopsis, Table of content graphic
35x13mm (600 x 600 DPI)